Electronic Companion for "Adaptive Preference Elicitation in Preference Robust CPT-Based Shortfall"

EC.1. Properties of the Preference Functional $\mathbb{E}_{g_1 g_2}[v(\cdot)]$

Before proving Proposition 1 in Section EC.2, we establish two preliminary lemmas analyzing the properties of the preference functional $\mathbb{E}_{g_1 g_2}[v(\cdot)]$ defined as in (2).

LEMMA EC.1. *Let $\mathbb{E}_{g_1 g_2}[v(\cdot)]$ be defined as in (2). Then*

$$\mathbb{E}_{g_1 g_2}[v(\eta)] \leq \mathbb{E}_{g_1 g_2}[v(\xi)],\ \forall \eta, \xi \in \mathcal{L}^\infty(\mathbb{R}) \text{ with } \eta(\omega) \leq \xi(\omega),\ \forall \omega \in \Omega.$$

Proof. By definition (see (2)),

$$\mathbb{E}_{g_1 g_2}[v(\xi)] = \int_0^\infty g_2(\mathbb{P}(v(\xi) > t))dt + \int_0^\infty -g_1(\mathbb{P}(-v(\xi) \geq t))dt.$$

Since $\eta(\omega) \leq \xi(\omega)$ for all $\omega \in \Omega$ and $v(\cdot)$ is monotonically increasing, $v(\eta(\omega)) \leq v(\xi(\omega))$ for all $\omega \in \Omega$, and consequently

$$\mathbb{P}(v(\eta) > t) \leq \mathbb{P}(v(\xi) > t) \quad \text{and} \quad \mathbb{P}(-v(\eta) \geq t) \geq \mathbb{P}(-v(\xi) \geq t).$$

Moreover, since g_1, g_2 are increasing, we have

$$g_2(\mathbb{P}(v(\eta) > t)) \leq g_2(\mathbb{P}(v(\xi) > t)) \quad \text{and} \quad -g_1(\mathbb{P}(-v(\eta) \geq t)) \leq -g_1(\mathbb{P}(-v(\xi) \geq t)).$$

A combination of the inequalities gives rise to $\mathbb{E}_{g_1 g_2}[v(\eta)] \leq \mathbb{E}_{g_1 g_2}[v(\xi)]$. The proof is complete.

□

LEMMA EC.2. *Let $\mathbb{E}_{g_1 g_2}[v(\cdot)]$ be defined as in (2) and $\xi \in \mathcal{L}^\infty(\mathbb{R})$. Then the following assertions hold.*

(i) For any $a, b \in \mathbb{R}$ with $a \leq b$,

$$\mathbb{E}_{g_1 g_2}[v(\xi - a)] \geq \mathbb{E}_{g_1 g_2}[v(\xi - b)].$$

(ii) For any $a, b \in \mathbb{R}$ with $a < b$,

$$\mathbb{E}_{g_1 g_2}[v(\xi - a)] > \mathbb{E}_{g_1 g_2}[v(\xi - b)].$$

Proof. Part (i) follows directly from Lemma EC.1.

Part (ii). Let $\Omega_1 := \{\omega \in \Omega : \xi(\omega) < b\}$. For a real number $a \in \mathbb{R}$, let $(a)_+ := \max\{a, 0\}$ and $(a)_- := \min\{a, 0\}$. For any $a < b$, we have

$$\xi(\omega) - b < [\xi(\omega) - a]_-, \ \forall \omega \in \Omega_1 \quad \text{and} \quad \xi(\omega) - b < [\xi(\omega) - a]_+, \ \forall \omega \in \Omega \backslash \Omega_1.$$

Since the value function $v \in \mathscr{V}$ is strictly increasing,

$$v^-(\xi(\omega) - b) < v^-([\xi(\omega) - a]_-), \ \forall \omega \in \Omega_1 \quad \text{and} \quad v^+(\xi(\omega) - b) < v^+([\xi(\omega) - a]_+), \ \forall \omega \in \Omega \backslash \Omega_1.$$

By the definition of $\mathbb{E}_{g_1 g_2}[v(\cdot)]$, we have

$$\mathbb{E}_{g_1 g_2}[v(\xi - b)] = \int_{-\infty}^{b} v^-(u - b)\, d\big(g_1(F_\xi(u))\big) + \int_{b}^{\infty} v^+(u - b)\, d\big(1 - g_2(1 - F_\xi(u))\big).$$

Since we have either $\mathbb{P}(\Omega_1) > 0$ or $\mathbb{P}(\Omega \backslash \Omega_1) > 0$ or both,

$$\begin{aligned}
\mathbb{E}_{g_1 g_2}[v(\xi - b)] &< \int_{-\infty}^{b} v^-([u - a]_-) d(g_1(F_\xi(u))) + \int_{b}^{\infty} v^+([u - a]_+) d(1 - g_2(1 - F_\xi(u))) \\
&\leq \int_{-\infty}^{a} v^-(u - a) d(g_1(F_\xi(u))) + \int_{a}^{\infty} v^+(u - a) d(1 - g_2(1 - F_\xi(u))) \\
&= \mathbb{E}_{g_1 g_2}[v(\xi - a)].
\end{aligned}$$

The proof is complete. □

EC.2. Proof of Proposition 1

Proof of Proposition 1. To simplify the exposition, we call x admissible for (4) if $\mathbb{E}_{g_1 g_2}[v(\xi - x)] \leq 0$, and admissible for (6) if $\sup_{(v, g_1, g_2) \in \mathbb{V}\mathbb{G}_1\mathbb{G}_2} \mathbb{E}_{g_1 g_2}[v(\xi - x)] \leq 0$. We begin by showing that the equality (7) holds when one of the quantities is $+\infty$. First, consider the case that $\rho_{\mathbb{V}\mathbb{G}_1\mathbb{G}_2}(\xi) = +\infty$. Then the admissible set corresponding to (6) is empty. Assume for the sake of a contradiction that $\hat{x} := \Pi_{\mathbb{V}\mathbb{G}_1\mathbb{G}_2}(\xi) < +\infty$. Then $\rho_{v, g_1, g_2}(\xi) \leq \hat{x} < +\infty$ for all $(v, g_1, g_2) \in \mathbb{V}\mathbb{G}_1\mathbb{G}_2$. Thus, for any positive number ϵ, it follows by Lemma EC.2 (i) that

$$\mathbb{E}_{g_1 g_2}[v(\xi - \hat{x} - \epsilon)] \leq \mathbb{E}_{g_1 g_2}[v(\xi - \rho_{v, g_1, g_2}(\xi) - \epsilon)] \leq 0, \ \forall (v, g_1, g_2) \in \mathbb{V}\mathbb{G}_1\mathbb{G}_2.$$

The latter implies $\hat{x} + \epsilon$ is admissible for (6), a contradiction.

Conversely, consider the case that $\Pi_{\mathbb{V}\mathbb{G}_1\mathbb{G}_2}(\xi) = +\infty$. Assume for a contradiction that $x^* := \rho_{\mathbb{V}\mathbb{G}_1\mathbb{G}_2}(\xi) < +\infty$. Then for any positive number ϵ, $x^* + \epsilon$ is admissible for (6), that is,

$$\sup_{(v, g_1, g_2) \in \mathbb{V}\mathbb{G}_1\mathbb{G}_2} \mathbb{E}_{g_1 g_2}[v(\xi - x^* - \epsilon)] \leq 0,$$

which implies

$$\mathbb{E}_{g_1g_2}[v(\xi - x^* - \epsilon)] \le 0,\ \forall (v, g_1, g_2) \in \mathbb{V}\mathbb{G}_1\mathbb{G}_2.$$

The latter guarantees that $\rho_{v,g_1,g_2}(\xi) \le x^* + \epsilon, \forall (v, g_1, g_2) \in \mathbb{V}\mathbb{G}_1\mathbb{G}_2$ and hence $\Pi_{\mathbb{V}\mathbb{G}_1\mathbb{G}_2}(\xi) \le x^* + \epsilon < +\infty$, a contradiction.

We now turn to discuss the case that the risk measures for ξ in (6) and (5) are both finite. Let x be admissible for (6). Then x is also admissible for (4) for any $(v, g_1, g_2) \in \mathbb{V}\mathbb{G}_1\mathbb{G}_2$, which implies $x^* \ge \hat{x}$.

Conversely, by definition, $\hat{x} \ge \rho_{v,g_1,g_2}(\xi)$ for any $(v, g_1, g_2) \in \mathbb{V}\mathbb{G}_1\mathbb{G}_2$. Thus, by Lemma EC.2(i), for any $\epsilon > 0$,

$$\mathbb{E}_{g_1g_2}[v(\xi - \hat{x} - \epsilon)] \le \mathbb{E}_{g_1g_2}[v(\xi - \rho_{v,g_1,g_2}(\xi) - \epsilon)] \le 0.$$

Hence, $\hat{x} + \epsilon$ is admissible for (6), implying $x^* \le \hat{x} + \epsilon$. Letting $\epsilon \downarrow 0$ yields $x^* \le \hat{x}$. □

EC.3. An Example of PRGSR-CPT with a Finite Ambiguity Set and Its Advantages

Example EC.1 (Worst CPT-Based Shortfall vs. PRGSR-CPT). Assume that the DM's preference can be represented by the CPT-based shortfall $\rho_{v,g_1,g_2}(\cdot)$. For two prospects $A = (p_1, x_1; \ldots; p_n, x_n)$ and $B = (q_1, y_1; \ldots; q_n, y_n)$, we have $\rho_{v,g_1,g_2}(A) < \rho_{v,g_1,g_2}(B)$.

Consider a simple case that the DM's preference may be represented by three triples of value and distortion functions $\{(v^i, g_1^i, g_2^i) : i = 1, 2, 3\}$. Suppose that (v^1, g_1^1, g_2^1) and (v^2, g_1^2, g_2^2) satisfy $\rho_{v^j,g_1^j,g_2^j}(A) < \rho_{v^j,g_1^j,g_2^j}(B)$, for $j = 1, 2$, but (v^3, g_1^3, g_2^3) does not. Then we define the ambiguity set as $\mathbb{V}\mathbb{G}_1\mathbb{G}_2 = \{(v^i, g_1^i, g_2^i) : i = 1, 2\}$. Let ξ be a random variable representing financial loss. Then the worst (largest) CPT-based shortfall of ξ is defined as

$$\Pi_{\mathbb{V}\mathbb{G}_1\mathbb{G}_2}(\xi) := \max_{i=1,2} \rho_{v^i,g_1^i,g_2^i}(\xi) \tag{EC.1}$$

and the PRGSR-CPT is defined as $\rho_{\mathbb{V}\mathbb{G}_1\mathbb{G}_2}(\xi) := \inf_{x \in \mathbb{R}} \left\{ x : \max_{i=1,2} \mathbb{E}_{g_1^i g_2^i}[v^i(\xi - x)] \le 0 \right\}$.

Remark EC.1 (Advantages of PRGSR-CPT). (i) In practice, the ambiguity set $\mathbb{V}\mathbb{G}_1\mathbb{G}_2$ is not a finite set, and consequently, $\Pi_{\mathbb{V}\mathbb{G}_1\mathbb{G}_2}(\xi)$ is computationally challenging to evaluate. To alleviate this difficulty, we use the equivalence between $\Pi_{\mathbb{V}\mathbb{G}_1\mathbb{G}_2}(\xi)$ and $\rho_{\mathbb{V}\mathbb{G}_1\mathbb{G}_2}(\xi)$ in Proposition 1 to reformulate the constraint function of PRGSR-CPT into a bilinear program when the ambiguity sets admit a linear structure (see Section 3).

(ii) We confine our study to the case that $[\underline{x}, \bar{x}]$ satisfies $\underline{x} < 0 < \bar{x}$, since we choose $v(0)$ as the maximal tolerable distorted expectation of $\xi - x$ in (4). Suppose that the DM has a reference point or benchmark in wealth denoted by $B \neq 0$. In this case, the distorted expectation of the value function is $\mathbb{E}^B_{g_1 g_2}[v(\xi)] := \int_B^{+\infty} v(x-B)d(-g_2(1-F_\xi(x))) + \int_{-\infty}^B v(x-B)d(g_1(F_\xi(x)))$, where $v \in \mathscr{V}$, $g_i \in \mathscr{G}$, for $i = 1, 2$. If we are able to estimate a bound $c > 0$ for $|\xi - x|$, then we can set $[\underline{x}, \bar{x}] = [-B-c, -B+c]$. Subsequently, we may replace $v(0)$ in the right-hand side of (4) with $v(-B) \neq 0$.

EC.4. Proof of Proposition 2

Proof of Proposition 2. By Proposition 1,

$$\rho_{\mathbb{V}\mathbb{G}_1\mathbb{G}_2^{\mathrm{con}}}(\xi) = \sup_{(v,g_1,g_2)\in\mathbb{V}\mathbb{G}_1\mathbb{G}_2^{\mathrm{con}}} \rho_{v,g_1,g_2}(\xi).$$

By Mao and Cai (2018, Corollary 2.8), $\rho_{v,g_1,g_2}(\cdot)$ is a convex risk measure if and only if $g_1(p)$ and $1-g_2(1-p)$ are convex in $p \in [0,1]$, and v is convex on both $\mathbb{R}_-$ and $\mathbb{R}_+$, and (v, g_1, g_2) satisfies the inequality in (8). Hence, $\mathcal{R}_{\mathrm{con}} = \{\rho_{v,g_1,g_2} : (v, g_1, g_2) \in \mathbb{V}\mathbb{G}_1\mathbb{G}_2^{\mathrm{con}}\}$. Taking the supremum over identical index sets yields

$$\rho_{\mathbb{V}\mathbb{G}_1\mathbb{G}_2^{\mathrm{con}}}(\xi) = \rho_{\mathcal{R}_{\mathrm{con}}}(\xi).$$

The proof is complete. □

EC.5. Proof of Proposition 3

Proof of Proposition 3. By Mao and Cai (2018, Theorem 2.10), $\rho_{v,g_1,g_2}(\cdot)$ is coherent if and only if $v \in \mathcal{V}_{\mathrm{coh}}$ and $g_1(p)$ and $1-g_2(1-p)$ are convex, and $\Upsilon(p) := a_1(1-g_2(1-p)) - a_2 g_1(p)$ is nondecreasing on $[0,1]$. Hence, $\mathcal{R}_{\mathrm{coh}} = \{\rho_{v,g_1,g_2} : (v, g_1, g_2) \in \mathbb{V}\mathbb{G}_1\mathbb{G}_2^{\mathrm{coh}}\}$. Moreover, it follows by Proposition 1 that $\rho_{\mathbb{V}\mathbb{G}_1\mathbb{G}_2^{\mathrm{coh}}}(\xi)$ can be rewritten as $\sup_{(v,g_1,g_2)\in\mathbb{V}\mathbb{G}_1\mathbb{G}_2^{\mathrm{coh}}} \rho_{v,g_1,g_2}(\xi)$. Taking the supremum over identical index sets yields

$$\Pi_{\mathbb{V}\mathbb{G}_1\mathbb{G}_2^{\mathrm{coh}}}(\xi) = \rho_{\mathcal{R}_{\mathrm{coh}}}(\xi).$$

The proof is complete. □

EC.6. Explanation of Strong Risk Taking in Remark 1

We will show that (i) the relation in (9) is equivalent to $\frac{v'_+(0)}{v'_-(0)} \geq \sup_{s\in(0,1)} \frac{g'_{1,-}(s)}{g'_{2,-}(1-s)}$; (ii) the positive homogeneity of CPT implies that the value function v is positively homogeneous.

(i) Note that the CPT value for the prospect $(p_1, x_1; \ldots; p_n, x_n)$ is evaluated by the functional $\mathrm{CPT}(p_1, x_1; \cdots; p_n, x_n) = \sum_{j=1}^{n} \pi_j v(x_j)$, where v is the value function, and π_j, $j = 1, \ldots, n$, are defined as

$$\pi_j = \begin{cases} g_2(p_1 + \cdots + p_j) - g_2(p_1 + \cdots + p_{j-1}) \text{ if } j \le k, \\ g_1(p_j + \cdots + p_n) - g_1(p_{j+1} + \cdots + p_n) \text{ if } j > k, \end{cases}$$

where $k \in \{0, \cdots, n\}$ satisfies $x_1 \ge \cdots \ge x_k \ge 0 > x_{k+1} \ge \cdots \ge x_n$. The relation in (9) is equivalent to the inequality expressed in terms of CPT-values:

$$\begin{aligned} &\sum_{j=1}^{k} (g_2(p_1 + \cdots + p_j) - g_2(p_1 + \cdots + p_{j-1}))v(x_j) \\ &\quad + \sum_{j=k+1}^{n} (g_1(p_j + \cdots + p_n) - g_1(p_{j+1} + \cdots + p_n))v(x_j) \\ &\quad \le \sum_{l=1, l\neq i}^{k} (g_2(p_1 + \cdots + p_l) - g_2(p_1 + \cdots + p_{l-1}))v(x_l) \\ &\qquad + \sum_{l=k+1, l\neq j}^{n} (g_1(p_l + \cdots + p_n) - g_1(p_{l+1} + \cdots + p_n))v(x_l) \\ &\qquad + (g_2(p_1 + \cdots + p_i) - g_2(p_1 + \cdots + p_{i-1}))v\left(x_i + \frac{\delta}{p_i}\right) \\ &\qquad + (g_1(p_j + \cdots + p_n) - g_1(p_{j+1} + \cdots + p_n))v\left(x_j - \frac{\delta}{p_j}\right), \end{aligned}$$

which reduces to

$$\begin{aligned} 0 \le &(g_2(p_1 + \cdots + p_i) - g_2(p_1 + \cdots + p_{i-1}))\left(v\left(x_i + \frac{\delta}{p_i}\right) - v(x_i)\right) \\ &+ (g_1(p_j + \cdots + p_n) - g_1(p_{j+1} + \cdots + p_n))\left(v\left(x_j - \frac{\delta}{p_j}\right) - v(x_j)\right). \end{aligned}$$

Let $p = p_i$, $q = p_j$, $r = p_1 + \ldots + p_{i-1}$ and $s = p_{j+1} + \ldots + p_n$. Then the inequality becomes

$$(g_1(s+q) - g_1(s))\left(v(x_j) - v\left(x_j - \frac{\delta}{q}\right)\right) \le (g_2(p+r) - g_2(r))\left(v\left(x_i + \frac{\delta}{p}\right) - v(x_i)\right),$$

which can be rewritten as

$$\frac{v(x_i + \frac{\delta}{p}) - v(x_i)}{v(x_j) - v(x_j - \frac{\delta}{q})} \ge \frac{g_1(s+q) - g_1(s)}{g_2(p+r) - g_2(r)}. \tag{EC.2}$$

Since v is convex over $\mathbb{R}_+$ and $\mathbb{R}_-$, $\frac{v(x_i+\frac{\delta}{p}) - v(x_i)}{\delta/p}$ decreases as $x_i \downarrow 0$ and $\delta \downarrow 0$, approaching its infimum $v'_+(0)$, and $\frac{v(x_j) - v(x_j - \frac{\delta}{q})}{\delta/q}$ increases as $x_j \uparrow 0$ and $\delta \downarrow 0$, approaching the supremum $v'_-(0)$. Thus, the

left-hand side of (EC.2) has an infimum of $\frac{v'_+(0)}{v'_-(0)}\frac{q}{p}$. Since g_2 is concave, $\frac{g_2(p+r)-g_2(r)}{p} \geq g'_{2,-}(p+r)$. Likewise, since g_1 is convex, we have $\frac{g_1(s+q)-g_1(s)}{q} \leq g'_{1,-}(s+q)$, where $g'_{2,-}(p+r)$ and $g'_{1,-}(s+q)$ denote the left derivatives of g_2 at $p+r$ and of g_1 at $s+q$, respectively. Thus, the right-hand side of (EC.2) is bounded above by $\frac{g'_{1,-}(s+q)}{g'_{2,-}(p+r)}\frac{q}{p}$. Summarizing the above discussion, (EC.2) holds if

$$\frac{v'_+(0)}{v'_-(0)} \geq \frac{g'_{1,-}(s+q)}{g'_{2,-}(p+r)}, \ \forall s+q \in (0,1). \tag{EC.3}$$

We now establish the following necessary and sufficient condition for (EC.2):

$$\frac{v'_+(0)}{v'_-(0)} \geq \sup_{\eta\in(0,1)} \frac{g'_{1,-}(\eta)}{g'_{2,-}(1-\eta)}. \tag{EC.4}$$

To establish sufficiency, observe that $p+r \leq 1-(s+q)$. By the concavity of g_2, $g'_{2,-}(p+r) \geq g'_{2,-}(1-(s+q))$. Hence, (EC.4) implies (EC.3). To establish necessity, consider adjacent outcomes with $j = i+1$, for which $p+r = 1-(s+q)$, and let $p, q \downarrow 0$. The resulting derivative ratios in (EC.2), together with $g'_{1,+} \geq g'_{1,-}$ by the convexity of g_1,yield (EC.4). Finally, $g'_{2,-}(1-\eta) = (1-g_2(1-\cdot))'_+(\eta)$.

(ii) Observe that $r\text{CPT}(p_1,x_1;\cdots;p_n,x_n) = \text{CPT}(p_1,rx_1;\cdots;p_n,rx_n)$ can be rewritten in terms of CPT values:

$$\begin{aligned}
&\sum_{j=1}^{k}(g_2(p_1+\cdots+p_j)-g_2(p_1+\cdots+p_{j-1}))rv(x_j)\\
&\quad+\sum_{j=k+1}^{n}(g_1(p_j+\cdots+p_n)-g_1(p_{j+1}+\cdots+p_n))rv(x_j)\\
&=\sum_{j=1}^{k}(g_2(p_1+\cdots+p_j)-g_2(p_1+\cdots+p_{j-1}))v(rx_j)\\
&\quad+\sum_{j=k+1}^{n}(g_1(p_j+\cdots+p_n)-g_1(p_{j+1}+\cdots+p_n))v(rx_j).
\end{aligned}$$

Considering the certain prospect $(1,x_j)$ for each $j=1,\ldots,n$, the positive homogeneity of CPT gives

$$rv(x_j) = v(rx_j), \ \forall j = 1,\cdots,n.$$

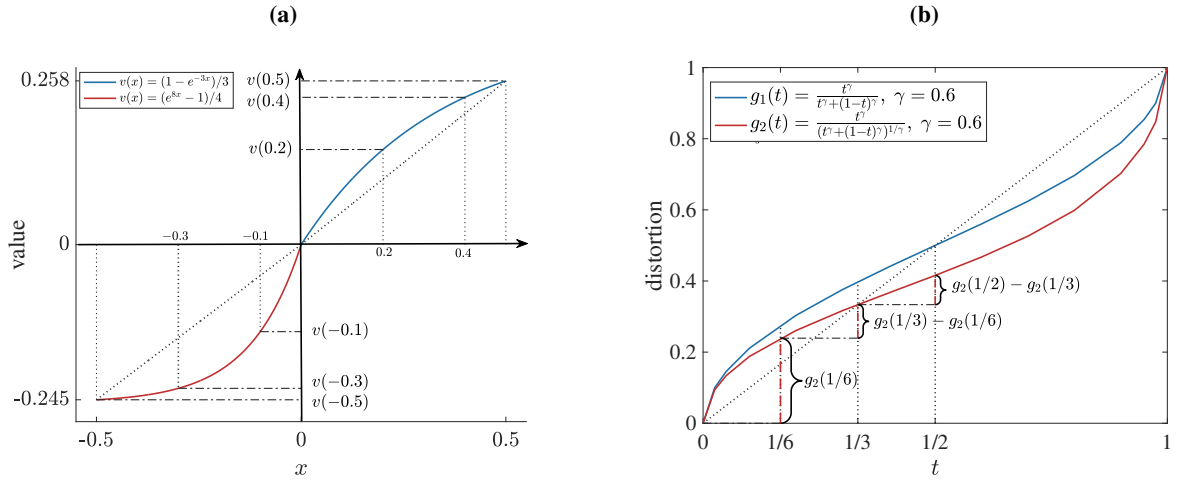
Thus, v is positively homogeneous.

EC.7. An Example of Calculating $\mathbb{E}_{g_1 g_2}[v(\xi - x)]$

We now illustrate the computation of $\mathbb{E}_{g_1 g_2}[v(\xi - x)]$ presented in Section 3.1.

EXAMPLE EC.2. Consider the value function v and the distortion functions g_1, g_2 as in Figure EC.1.

Figure EC.1 **(a)** Example of the value function (nonsmooth at 0). **(b)** Example of the distortion functions.



To see how the distorted expectation $\mathbb{E}_{g_1 g_2}[v(\xi - x)]$ is computed, let ξ be a random variable with $P(\xi = -0.1) = 1/6$, $P(\xi = 0.2) = 1/6$, $P(\xi = -0.3) = 1/6$, $P(\xi = 0.4) = 1/6$, $P(\xi = -0.5) = 1/6$, $P(\xi = 0.5) = 1/6$ and $x = 0$. Then from Tables EC.1–EC.2,

$$\begin{aligned} h^1_{g_1 g_2}[v(\xi - x)] =& v(-0.5)g_1(1/6) + v(-0.3)\Big(g_1(1/3) - g_1(1/6)\Big) + v(-0.1)\Big(g_1(1/2) - g_1(1/3)\Big) \\ \approx& -0.0677 - 0.0277 - 0.0141 = -0.1095, \\ h^2_{g_1 g_2}[v(\xi - x)] =& v(0.2)\Big(g_2(1/2) - g_2(1/3)\Big) + v(0.4)\Big(g_2(1/3) - g_2(1/6)\Big) + v(0.5)g_2(1/6) \\ \approx& 0.0124 + 0.0220 + 0.0619 = 0.0963. \end{aligned}$$

Then $\mathbb{E}_{g_1 g_2}[v(\xi - x)] = h^1_{g_1 g_2}[v(\xi - x)] + h^2_{g_1 g_2}[v(\xi - x)] \approx -0.0132$.

Table EC.1 Distorted probabilities for Losses

Order No. k	1	2	3
Loss $\xi_k < 0$	-0.5	-0.3	-0.1
q_k	$q_1 = 1/6$	$q_2 = 1/3$	$q_3 = 1/2$
Distorted probability	$g_1(q_1) - g_1(q_0)$ $= g_1(1/6)$	$g_1(q_2) - g_1(q_1)$ $= g_1(1/3) - g_1(1/6)$	$g_1(q_3) - g_1(q_2)$ $= g_1(1/2) - g_1(1/3)$

Table EC.2 Distorted Probabilities for Gains

Order No. k	4	5	6
Gain $\xi_k > 0$	0.2	0.4	0.5
q_k	$q_4 = 2/3$	$q_5 = 5/6$	$q_6 = 1$
Distorted probability	$g_2(1-q_3) - g_2(1-q_4)$ $= g_2(1/2) - g_2(1/3)$	$g_2(1-q_4) - g_2(1-q_5)$ $= g_2(1/3) - g_2(1/6)$	$g_2(1-q_5) - g_2(1-q_6)$ $= g_2(1/6)$

EC.8. Bisection Method for Computing the CPT-based Shortfall (4)

We present a general form of the bisection method. Suppose that based on the minimal and maximal values of ξ and the monotonicity of the mapping $t \mapsto \mathbb{E}_{g_1 g_2}[v(\xi - t)]$, we can obtain a lower bound t_l^0 and an upper bound t_u^0 for the CPT-based shortfall risk measure t^*: $\rho_{v,g_1,g_2}(\xi) = \inf\{t \in \mathbb{R} : \mathbb{E}_{g_1 g_2}[v(\xi - t)] \le 0\}$, i.e., $\rho_{v,g_1,g_2}(\xi) = t^*$, where $t_l^0 \le t^* \le t_u^0$. Then we can carry out the bisection search to find t^*.

Algorithm 1 Bisection method for computing $\rho_{v,g_1,g_2}(\xi)$

Step 0. Set $k := 0$. Set $t_l := t_l^0$ and $t_u := t_u^0$.

Step 1. Set $t_k := \frac{t_l + t_u}{2}$ and compute $s := \mathbb{E}_{g_1 g_2}[v(\xi - t_k)]$. If $s < 0$, then update $t_u := t_k$ and $t_l := t_l$; if $s > 0$, then update $t_l := t_k$ and $t_u := t_u$; stop if $s = 0$.

Step 2. Set $k := k + 1$ and go to Step 1.

EC.9. Proof of Proposition 4

Proof of Proposition 4. Observe that $r_1^m, r_2^m, r_3^m \in \mathcal{J}$ and $1 - p^m \in \mathcal{S}_1$, and $p^m \in \mathcal{S}_2$ for $m \in [M]$. By construction in (27), v_J coincides with v on $\mathcal{J}$ and g_{iN_i} coincides with g_i on $\mathcal{S}_i$. It follows by (12) and (27) that

$$\begin{aligned}
\mathbb{E}_{g_{1N_1} g_{2N_2}}[v_J(Z_1^m)] =& v_J(r_1^m)\big(g_{1N_1}(1-p^m)\mathbb{1}_{r_1^m<0} + (1 - g_{2N_2}(p^m))\mathbb{1}_{r_1^m \ge 0}\big) \\
&+ v_J(r_3^m)\big((1 - g_{1N_1}(1-p^m))\mathbb{1}_{r_3^m<0} + g_{2N_2}(p^m)\mathbb{1}_{r_3^m \ge 0}\big) \\
=& v(r_1^m)\big(g_1(1-p^m)\mathbb{1}_{r_1^m<0} + (1 - g_2(p^m))\mathbb{1}_{r_1^m \ge 0}\big) \\
&+ v(r_3^m)\big((1 - g_1(1-p^m))\mathbb{1}_{r_3^m<0} + g_2(p^m)\mathbb{1}_{r_3^m \ge 0}\big) = \mathbb{E}_{g_1 g_2}[v(Z_1^m)],
\end{aligned} \tag{EC.5}$$

and $\mathbb{E}_{g_{1N_1} g_{2N_2}}[v_J(Z_2^m)] = v_J(r_2^m) = v(r_2^m) = \mathbb{E}_{g_1 g_2}[v(Z_2^m)]$, $m \in [M]$. The relation means that under the specific structures of v_J and g_{iN_i}, the distorted expected value of $v_J(Z_i^m)$ based on g_{iN_i} coincides with the distorted expected value of $v(Z_i^m)$ based on g_1, g_2. This shows $(v_J, g_{1N_1}, g_{2N_2}) \in \mathbb{V}_J \mathbb{G}_{N_1} \mathbb{G}_{N_2}$ as desired. □

EC.10. Three Types of Inconsistency

Let $\mathrm{CPT}(X) = \mathbb{E}_{g_1 g_2}[v(X)]$ for a random variable $X \in \mathcal{L}^\infty(\mathbb{R})$. We distinguish three sources of inconsistency in preference elicitation.

(1) The evaluation of the CPT values of the random variables (lotteries) contains noise. Instead of having $\mathrm{CPT}(X_m) - \mathrm{CPT}(Y_m) \le 0$, the errors in the evaluation of $\mathrm{CPT}(X_m)$ and/or $\mathrm{CPT}(Y_m)$ may lead to $\mathrm{CPT}(X_m) - \mathrm{CPT}(Y_m) > 0$. To address the issue, we may introduce a positive number $\gamma_m > 0$ such that if $\mathrm{CPT}(X_m) - \mathrm{CPT}(Y_m) \le \gamma_m$. By setting a bound on the total errors, we may consider the ambiguity set

$$\left\{ (v, g_1, g_2) \in \mathscr{V} \times \mathscr{G} \times \mathscr{G} : \exists\, \gamma_m \ge 0,\ \mathrm{CPT}(X_m) - \mathrm{CPT}(Y_m) \le \gamma_m,\ m \in [M],\ \sum_{m=1}^{M} \gamma_m \le \Gamma \right\}.$$

This kind of approach is widely used in the literature of PRO (see Armbruster and Delage 2015, Guo et al. 2024).

(2) The second type of error occurs in the perception of the outcomes of lotteries (Armbruster and Delage 2015). Specifically, the random variable X is perceived as $X + \delta$. If $\delta_{\min} \le \delta \le \delta_{\max}$ almost surely, then we could replace the condition $\mathrm{CPT}(X_m) - \mathrm{CPT}(Y_m) \le 0$ with $\mathrm{CPT}(X_m + \delta_{\min}) - \mathrm{CPT}(Y_m + \delta_{\max}) \le 0$. Let $\mathcal{U} := \mathscr{V}_{\mathrm{S}} \times \mathscr{G}^1_{\mathrm{invS}} \times \mathscr{G}^2_{\mathrm{invS}}$. In the case when $\delta_{\min} < 0$ and $\delta_{\max} > 0$, the latter is a relaxation of the former due to the monotonicity of the CPT functional. In our formulations $\mathbb{E}_{g_1 g_2}[v(X_m)] \le \mathbb{E}_{g_1 g_2}[v(Y_m)]$, for $m \in [M]$, we would need to replace X_m with $X_m + \delta_{\min}$ and Y_m with $Y_m + \delta_{\max}$, and the ambiguity set is replaced by

$$(\mathbb{V}\mathbb{G}_1\mathbb{G}_2)_M = \left\{ (v, g_1, g_2) \in \mathcal{U} : \mathbb{E}_{g_1 g_2}[v(X_m + \delta_{\min})] \le \mathbb{E}_{g_1 g_2}[v(Y_m + \delta_{\max})],\ m \in [M] \right\}.$$

(3) The third type of error potentially arises from the DM's wrong responses to the elicitation query. In the spirit of Bertsimas and O'Hair (2013), we may allow at most ϵM of the total M pairwise comparisons to be mistaken (receiving wrong answers from the DM), in which case at most $100(1-\epsilon)\%$ of the M pairwise comparisons are correct. In that case, we can introduce binary variables δ_m with $\delta_m = 1$ if the DM is mistaken about lottery m and 0 otherwise. Consequently, we can replace the condition $\mathrm{CPT}(X_m) \le \mathrm{CPT}(Y_m)$ with the two inequalities

$$\mathrm{CPT}(X_m) \le \mathrm{CPT}(Y_m) + \delta_m \mathcal{M} \quad \text{and} \quad \mathrm{CPT}(Y_m) \le \mathrm{CPT}(X_m) + (1 - \delta_m)\mathcal{M},$$

where $\mathcal{M}$ is a large constant ("big M"), and we require $\sum_{m=1}^{M} \delta_m \le \epsilon M$.

Next, we present an example which shows that the true preference function is excluded from the constructed ambiguity set when we use the wrong model (EUT, DRM or RDEU) to construct the set of preference functions (value function and/or distortion function), whereas CPT describes the DM's preference.

EXAMPLE EC.3 (PREFERENCE INCONSISTENCY WITH EUT, DRM AND RDEU). We consider a risky lottery Z_1 and a certain lottery Z_2 as defined in (11) with parameters $r_1 \in [-0.5, 0)$, $r_3 \in (0, 0.5]$, $r_2 \in [-0.5, 0.5]$, and $p \in (0, 1)$. The true utility function v^* and distortion functions g_1^*, g_2^* are the same as those in Example 1. The preference relation between Z_1 and Z_2 under the preference functional $\rho(\cdot)$ can be quantified by the inequality $h(\rho(Z_1) - \rho(Z_2)) \le 0$, where $h = 1$ when $Z_1 \preceq Z_2$, and $h = -1$ otherwise. Here $\rho(\cdot)$ may represent $\rho_{\text{EUT}}(\cdot) := \mathbb{E}[v^*(\cdot)]$, $\rho_{\text{DRM}}(\cdot) := \mathbb{E}_{g_1^*}[\cdot]$, $\rho_{\text{RDEU}}(\cdot) := \mathbb{E}_{g_1^*}[v^*(\cdot)]$, and $\rho_{\text{CPT}}(\cdot) := \mathbb{E}_{g_1^* g_2^*}[v^*(\cdot)]$, under EUT, DRM, RDEU, and CPT, respectively. We assume that the preference of the DM follows CPT. Preference inconsistency may occur when we use EUT, DRM, or RDEU to describe the DM's preference in the following three cases.

1. Take $(r_1, r_2, r_3, p) = (-0.15, 0.008, 0.25, 0.4)$. Under CPT, $\mathbb{E}_{g_1^* g_2^*}[v^*(Z_1)] - \mathbb{E}_{g_1^* g_2^*}[v^*(Z_2)] = 0.0083 \ge 0$, and hence the DM's response to this query is $Z_2 \preceq Z_1$, $h = -1$, and

$$\underline{\rho_{\text{EUT}}(Z_1) - \rho_{\text{EUT}}(Z_2) = -0.0015 \le 0} \quad \text{and} \quad \rho_{\text{DRM}}(Z_1) - \rho_{\text{DRM}}(Z_2) = 0.0063 \ge 0, \tag{EC.6a}$$

$$\rho_{\text{RDEU}}(Z_1) - \rho_{\text{RDEU}}(Z_2) = 0.0021 \ge 0 \quad \text{and} \quad \rho_{\text{CPT}}(Z_1) - \rho_{\text{CPT}}(Z_2) = 0.0083 \ge 0. \tag{EC.6b}$$

Based on the responses of the DM and under the framework of the EUT, we can use the inequality $\rho_{\text{EUT}}(Z_1) - \rho_{\text{EUT}}(Z_2) \ge 0$ to construct the set S_1 of utility functions, i.e., $S_1 = \{v : v(r_1)(1-p) + v(r_3)p - v(r_2) \ge 0\}$. However, the true utility satisfies the inequality (EC.6a), which has the opposite sign to the inequality defining S_1. Thus, the constructed set S_1 does not contain the true utility.

2. Take $(r_1, r_2, r_3, p) = (-0.5, 0.01, 0.1, 0.8)$. Under CPT, $\mathbb{E}_{g_1^* g_2^*}[v^*(Z_1)] - \mathbb{E}_{g_1^* g_2^*}[v^*(Z_2)] = 0.0183 \ge 0$, and hence the DM's response to this query is $Z_2 \preceq Z_1$, $h = -1$, and

$$\rho_{\text{EUT}}(Z_1) - \rho_{\text{EUT}}(Z_2) = 0.0391 \ge 0 \quad \text{and} \quad \underline{\rho_{\text{DRM}}(Z_1) - \rho_{\text{DRM}}(Z_2) = -0.0453 \le 0}, \tag{EC.7a}$$

$$\rho_{\text{RDEU}}(Z_1) - \rho_{\text{RDEU}}(Z_2) = 0.0290 \ge 0 \quad \text{and} \quad \rho_{\text{CPT}}(Z_1) - \rho_{\text{CPT}}(Z_2) = 0.0183 \ge 0. \tag{EC.7b}$$

Based on the responses of the DM and under the framework of DRM, we can use the inequality $\rho_{\text{DRM}}(Z_1) - \rho_{\text{DRM}}(Z_2) \ge 0$ to construct the set S_2 of distortion functions, i.e., $S_2 = \{g_1 : r_1 g_1(1 -$

$p)+r_3(1-g_1(1-p))-r_2\geq 0\}$. However, the true distortion satisfies the inequality (EC.7a), which has the opposite sign to the inequality defining S_2. Thus, the constructed set S_2 does not contain the true distortion.

3. Take $(r_1,r_2,r_3,p)=(-0.25,0.0195,0.25,0.55)$. Under CPT, $\mathbb{E}_{g_1^*g_2^*}[v^*(Z_1)]-\mathbb{E}_{g_1^*g_2^*}[v^*(Z_2)]=-0.0016\leq 0$, and hence the DM's response to this query is $Z_1\preceq Z_2$, $h=1$, and

$$\rho_{\mathrm{EUT}}(Z_1)-\rho_{\mathrm{EUT}}(Z_2)=0.00364\geq 0 \quad \text{and} \quad \rho_{\mathrm{DRM}}(Z_1)-\rho_{\mathrm{DRM}}(Z_2)=0.0027\geq 0, \tag{EC.8a}$$

$$\underline{\rho_{\mathrm{RDEU}}(Z_1)-\rho_{\mathrm{RDEU}}(Z_2)=0.0015\geq 0} \quad \text{and} \quad \rho_{\mathrm{CPT}}(Z_1)-\rho_{\mathrm{CPT}}(Z_2)=-0.0016\leq 0. \tag{EC.8b}$$

Based on the responses of the DM and under the framework of RDEU, we can use the inequality $\rho_{\mathrm{RDEU}}(Z_1)-\rho_{\mathrm{RDEU}}(Z_2)\leq 0$ to construct the set S_3 of utility functions and distortion functions, i.e., $S_3=\{(v,g_1): v(r_1)g_1(1-p)+v(r_3)(1-g_1(1-p))-v(r_2)\leq 0\}$. However, the true utility and distortion function satisfy the inequality (EC.8b), which has the opposite sign to the inequality defining S_3. Thus, the constructed set S_3 does not contain the true utility and true distortion functions.

EC.11. Proof of Theorem 1

Proof of Theorem 1. Part (i). Since $\mathbb{V}_J\mathbb{G}_{N_1}\mathbb{G}_{N_2}\subset\mathbb{V}\mathbb{G}_1\mathbb{G}_2$, by the definition of $h_{\mathbb{V}\mathbb{G}_1\mathbb{G}_2}$ in (22), for any fixed $x\in\mathbb{R}$,

$$h_{\mathbb{V}\mathbb{G}_1\mathbb{G}_2}(\xi-x)\geq h_{\mathbb{V}_J\mathbb{G}_{N_1}\mathbb{G}_{N_2}}(\xi-x). \tag{EC.9}$$

It suffices to show that $h_{\mathbb{V}\mathbb{G}_1\mathbb{G}_2}(\xi-x)\leq h_{\mathbb{V}_J\mathbb{G}_{N_1}\mathbb{G}_{N_2}}(\xi-x)$. Let ε be a small positive number, and $(v_\varepsilon^*,g_{1,\varepsilon}^*,g_{2,\varepsilon}^*)\in\mathbb{V}\mathbb{G}_1\mathbb{G}_2$ be such that

$$\mathbb{E}_{g_{1,\varepsilon}^*g_{2,\varepsilon}^*}[v_\varepsilon^*(\xi-x)]\geq \sup_{(v,g_1,g_2)\in\mathbb{V}\mathbb{G}_1\mathbb{G}_2}\mathbb{E}_{g_1g_2}[v(\xi-x)]-\varepsilon. \tag{EC.10}$$

By Proposition 4, we can find a tuple of PLFs $(v_{J,\varepsilon}^*,g_{1N_1,\varepsilon}^*,g_{2N_2,\varepsilon}^*)\in\mathbb{V}_J\mathbb{G}_{N_1}\mathbb{G}_{N_2}$ such that $v_{J,\varepsilon}^*(\xi_k-x)=v_\varepsilon^*(\xi_k-x)$, $k\in[K]$, $g_{1N_1,\varepsilon}^*(q_k)=g_{1,\varepsilon}^*(q_k)$ for $k\in[K_0(x)-1]$, and $g_{2N_2,\varepsilon}^*(1-q_k)=g_{2,\varepsilon}^*(1-q_k)$

for $k = K_0(x) - 1, \cdots, K$. Consequently, we have

$$\begin{aligned}
&\mathbb{E}_{g^*_{1N_1,\varepsilon} g^*_{2N_2,\varepsilon}}[v^*_{J,\varepsilon}(\xi - x)] \\
&\quad = \sum_{k=1}^{K_0(x)-1} v^*_{J,\varepsilon}(\xi_k - x)(g^*_{1N_1,\varepsilon}(q_k) - g^*_{1N_1,\varepsilon}(q_{k-1})) \\
&\qquad + \sum_{k=K_0(x)}^{K} v^*_{J,\varepsilon}(\xi_k - x)(g^*_{2N_2,\varepsilon}(1-q_{k-1}) - g^*_{2N_2,\varepsilon}(1-q_k)) \\
&\quad = \sum_{k=1}^{K_0(x)-1} v^*_{\varepsilon}(\xi_k - x)(g^*_{1,\varepsilon}(q_k) - g^*_{1,\varepsilon}(q_{k-1})) + \sum_{k=K_0(x)}^{K} v^*_{\varepsilon}(\xi_k - x)(g^*_{2,\varepsilon}(1-q_{k-1}) - g^*_{2,\varepsilon}(1-q_k)) \\
&\quad = \mathbb{E}_{g^*_{1,\varepsilon} g^*_{2,\varepsilon}}[v^*_{\varepsilon}(\xi - x)].
\end{aligned} \tag{EC.11}$$

It follows by (EC.10) and (EC.11) that

$$\begin{aligned}
\sup_{(v,g_1,g_2)\in \mathbb{V}_J \mathbb{G}_{N_1} \mathbb{G}_{N_2}} \mathbb{E}_{g_1 g_2}[v(\xi - x)] &\geq \mathbb{E}_{g^*_{1N_1,\varepsilon} g^*_{2N_2,\varepsilon}}[v^*_{J,\varepsilon}(\xi - x)] = \mathbb{E}_{g^*_{1,\varepsilon} g^*_{2,\varepsilon}}[v^*_{\varepsilon}(\xi - x)] \\
&\geq \sup_{(v,g_1,g_2)\in \mathbb{V}\mathbb{G}_1\mathbb{G}_2} \mathbb{E}_{g_1 g_2}[v(\xi - x)] - \varepsilon,
\end{aligned}$$

and hence

$$h_{\mathbb{V}_J \mathbb{G}_{N_1} \mathbb{G}_{N_2}}(\xi - x) \geq h_{\mathbb{V}\mathbb{G}_1\mathbb{G}_2}(\xi - x), \tag{EC.12}$$

because ε can be arbitrarily small. A combination of (EC.9) and (EC.12) yields

$$h_{\mathbb{V}\mathbb{G}_1\mathbb{G}_2}(\xi - x) = h_{\mathbb{V}_J \mathbb{G}_{N_1} \mathbb{G}_{N_2}}(\xi - x).$$

Part (ii). We begin by giving a finite-dimensional program representation of $h_{\mathbb{V}_J \mathbb{G}_{N_1} \mathbb{G}_{N_2}}(\xi - x)$. For a fixed $x \in \mathbb{R}$, we can write $h_{\mathbb{V}_J \mathbb{G}_{N_1} \mathbb{G}_{N_2}}(\xi - x)$ as

$$\begin{aligned}
h_{\mathbb{V}_J \mathbb{G}_{N_1} \mathbb{G}_{N_2}}(\xi - x) = \sup_{v_J, g_{1N_1}, g_{2N_2}} \quad & \mathbb{E}_{g_{1N_1} g_{2N_2}}[v_J(\xi - x)] \\
\text{s.t.} \quad & h_m(\mathbb{E}_{g_{1N_1} g_{2N_2}}[v_J(Z_1^m)] - v_J(r_2^m)) \leq 0, \ \forall m \in [M], \\
& v_J \in \mathscr{V}_{\mathrm{S}}^J, \ g_{iN_i} \in \mathscr{G}_{\mathrm{invS}}^{iN_i}, \ i = 1, 2.
\end{aligned} \tag{EC.13}$$

Recall that $v_J(x) = (x\boldsymbol{a} + \boldsymbol{b})^\top \boldsymbol{\phi}(x)$, and $g_{iN_i}(t) = \boldsymbol{\sigma}_i^\top \boldsymbol{h}^{S_i}(t)$, $i = 1, 2$ (see (14) and (15)). Based on Part (i), it suffices to reformulate problem (EC.13) in terms of $\boldsymbol{a}, \boldsymbol{b}, \boldsymbol{\sigma}_1$ and $\boldsymbol{\sigma}_2$. By (12), we obtain

$$\begin{aligned}
\mathbb{E}_{g_{1N_1} g_{2N_2}}[v_J(Z_1^m)] =& (r_1^m \boldsymbol{a} + \boldsymbol{b})^\top \boldsymbol{\phi}(r_1^m) \Big(\boldsymbol{\sigma}_1^\top \boldsymbol{h}^{S_1}(1 - p^m) \mathbb{1}_{r_1^m < 0} + (1 - \boldsymbol{\sigma}_2^\top \boldsymbol{h}^{S_2}(p^m)) \mathbb{1}_{r_1^m \geq 0} \Big) \\
&+ (r_3^m \boldsymbol{a} + \boldsymbol{b})^\top \boldsymbol{\phi}(r_3^m) \Big((1 - \boldsymbol{\sigma}_1^\top \boldsymbol{h}^{S_1}(1 - p^m)) \mathbb{1}_{r_3^m < 0} + \boldsymbol{\sigma}_2^\top \boldsymbol{h}^{S_2}(p^m) \mathbb{1}_{r_3^m \geq 0} \Big) \\
=& R^m(\boldsymbol{a}, \boldsymbol{b}, \boldsymbol{\sigma}_1, \boldsymbol{\sigma}_2),
\end{aligned}$$

and $\mathbb{E}_{g_{1N_1}g_{2N_2}}[v_J(Z_2^m)] = v_J(r_2^m) = (r_2^m\boldsymbol{a}+\boldsymbol{b})^\top\boldsymbol{\phi}(r_2^m)$. Thus, the inequalities $h_m(\mathbb{E}_{g_{1N_1}g_{2N_2}}[v_J(Z_1^m)] - \mathbb{E}_{g_{1N_1}g_{2N_2}}[v_J(Z_2^m)]) \le 0$ for $m \in [M]$ are equivalent to $h_m(R^m(\boldsymbol{a},\boldsymbol{b},\boldsymbol{\sigma}_1,\boldsymbol{\sigma}_2) - (r_2^m\boldsymbol{a}+\boldsymbol{b})^\top\boldsymbol{\phi}(r_2^m)) \le 0$ for $m \in [M]$, which is constraint (28k). On the other hand, by (10a), the objective function of $h_{\mathbb{V}_J\mathbb{G}_{N_1}\mathbb{G}_{N_2}}(\xi - x)$ takes the form

$$\begin{aligned}
\mathbb{E}_{g_{1N_1}g_{2N_2}}[v_J(\xi-x)] &= \sum_{k=1}^{K_0(x)-1} v_J(\xi_k - x)(g_{1N_1}(q_k) - g_{1N_1}(q_{k-1})) \\
&\quad + \sum_{k=K_0(x)}^{K} v_J(\xi_k - x)(g_{2N_2}(1-q_{k-1}) - g_{2N_2}(1-q_k)) \\
&= \sum_{k=1}^{K_0(x)-1} ((\xi_k - x)\boldsymbol{a}+\boldsymbol{b})^\top\boldsymbol{\phi}(\xi_k - x)\boldsymbol{\sigma}_1^\top(\boldsymbol{h}^{\mathcal{S}_1}(q_k) - \boldsymbol{h}^{\mathcal{S}_1}(q_{k-1})) \\
&\quad + \sum_{k=K_0(x)}^{K} ((\xi_k - x)\boldsymbol{a}+\boldsymbol{b})^\top\boldsymbol{\phi}(\xi_k - x)\boldsymbol{\sigma}_2^\top(\boldsymbol{h}^{\mathcal{S}_2}(1-q_{k-1}) - \boldsymbol{h}^{\mathcal{S}_2}(1-q_k)).
\end{aligned}$$

Thus, problem (28) provides an equivalent finite-dimensional reformulation of $h_{\mathbb{V}_J\mathbb{G}_{N_1}\mathbb{G}_{N_2}}(\xi - x)$ and the proof is complete. □

EC.12. Bisection Method for Computing PRGSR-CPT (6)

Algorithm 2 Bisection method for computing PRGSR-CPT (6)

Step 0. Set $k := 0$. Set $t_l := t_l^0$ and $t_u := t_u^0$.

Step 1. Set $t_k := \frac{t_l+t_u}{2}$ and compute $s := \sup_{(v,g_1,g_2)\in\mathbb{V}\mathbb{G}_1\mathbb{G}_2} \mathbb{E}_{g_1g_2}[v(\xi - t_k)]$. If $s < 0$, then update $t_u := t_k$; otherwise, update $t_l := t_k$.

Step 2. Set $k := k+1$ and go to Step 1.

EC.13. Proof of Proposition 5

Proof of Proposition 5 Since $\boldsymbol{c}_2^m > 0$ and $\boldsymbol{e}^\top\boldsymbol{c}_2^m < 1$, $(\boldsymbol{c}_2^m, 1-\boldsymbol{e}^\top\boldsymbol{c}_2^m) > 0$, which implies that the function $p \mapsto (\boldsymbol{R}\boldsymbol{c}_2^m)^\top\boldsymbol{h}^{\mathcal{S}_2}(p)$ is strictly increasing on $[0,1]$. Moreover, by the assumption that $(\widetilde{\boldsymbol{\sigma}}_2^{1m}, 1-\boldsymbol{e}^\top\widetilde{\boldsymbol{\sigma}}_2^{1m})$ has no zero component, it follows that $\{p^{m,i}\}$ is determined by $(\boldsymbol{R}\boldsymbol{c}_2^m)^\top\boldsymbol{h}^{\mathcal{S}_2}(p^{m,i}) = D_i$ in (35), for $i \in [N_2-2]$. Note that $\boldsymbol{h}^{\mathcal{S}_2}(p^{m,i}) = \Big(\underbrace{1,\cdots,1}_{j_i-1}, \frac{p^{m,i}-t_{j_i}}{t_{j_i+1}-t_{j_i}}, \underbrace{0,\cdots,0}_{N_2-1-j_i}\Big) \in \mathbb{R}^{N_2-1}$, for $p^{m,i} \in (t_{j_i}, t_{j_i+1}]$ with some $j_i \in [N_2-1]$. Observe that

$$(\boldsymbol{R}\boldsymbol{c}_2^m)^\top\boldsymbol{h}^{\mathcal{S}_2}(p^{m,i}) = \sum_{l=1}^{j_i-1} c_{2,l}^m + c_{2,j_i}^m \frac{p^{m,i}-t_{j_i}}{t_{j_i+1}-t_{j_i}}, \text{ for } p^{m,i} \in (t_{j_i}, t_{j_i+1}] \text{ with some } j_i \le N_2-2. \quad \text{(EC.14)}$$

Let $s \in [N_2 - 2]$. If $D_i = \sum_{j=1}^{s} c_{2,j}^m$ and $p^{m,i}$ satisfies $(\boldsymbol{R}\boldsymbol{c}_2^m)^\top \boldsymbol{h}^{\mathcal{S}_2}(p^{m,i}) = D_i$, then (EC.14) is equivalent to

$$\sum_{l=1}^{j_i-1} c_{2,l}^m + c_{2,j_i}^m \frac{p^{m,i} - t_{j_i}}{t_{j_i+1} - t_{j_i}} = \sum_{j=1}^{s} c_{2,j}^m,$$

which means $p^{m,i} = t_{s+1}$. The proof is complete. □

EC.14. RRUS versus the Modified Polyhedral Method

Example EC.4 (RRUS vs. the Modified Polyhedral Method). Consider the true utility function: $u^*(t) = 2(e^{8t} - 1)/8$, for $t \in [-0.5, 0]$ and $u^*(t) = (1 - e^{-3t})/3$ for $t \in [0, 0.5]$.

1. **Random Relative Utility Split Scheme**. We randomly generate 10 queries with a risky lottery Z_1^m and a deterministic lottery Z_2^m:

$$Z_1^m = \begin{cases} r_1^m \text{ w.p. } 1 - p^m \\ r_3^m \text{ w.p. } p^m \end{cases} \quad \text{and} \quad Z_2^m = r_2^m,$$

where the parameters (r_1^m, r_2^m, r_3^m) are given by

$$\begin{aligned}
&m = 1 : (-0.39389, -0.12723, 0.13943); && m = 2 : (-0.34508, 0.00218, 0.34945) \\
&m = 3 : (-0.02082, 0.08383, 0.18848); && m = 4 : (-0.47790, -0.12964, 0.21861) \\
&m = 5 : (-0.09662, 0.08570, 0.26803); && m = 6 : (-0.37031, -0.34015, -0.30999) \\
&m = 7 : (-0.31495, -0.27677, -0.23860); && m = 8 : (-0.36184, -0.09444, 0.17296) \\
&m = 9 : (-0.35396, -0.05848, 0.23700); && m = 10 : (-0.46137, -0.38929, -0.31721).
\end{aligned}$$

Next, we use RRUS to determine the parameter p^m. Specifically, let $\mathcal{X} = \{-0.5, 0, 0.5, r_1^m, r_2^m, r_3^m : m = 1, \ldots, 10\}$ be the set of breakpoints with $N = |\mathcal{X}| = 33$ and $\mathcal{U}_N$ be the set of all increasing piecewise linear utility functions defined over $[-0.5, 0.5]$ with breakpoints $\mathcal{X}$. Let $\mathcal{U}_N^0 = \mathcal{U}_N$. For (r_1^1, r_2^1, r_3^1), let $u_N(r_1^1) = 0$ and $u_N(r_3^1) = 1$. Then

$$\mathbb{E}[u_N(Z_1^1)] - \mathbb{E}[u_N(Z_2^1)] = (1 - p^1)u_N(r_1^1) + p^1 u_N(r_3^1) - u_N(r_2^1) = p^1 - u_N(r_2^1).$$

Let $I_1^1 = \min_{u_N \in \mathcal{U}_N^0} u_N(r_2^1)$ and $I_2^1 = \max_{u_N \in \mathcal{U}_N^0} u_N(r_2^1)$. Then $p^1 = 0.5(I_1^1 + I_2^1)$, and

$$\mathcal{U}_N^1 = \{u_N \in \mathcal{U}_N^0 : h_1((1 - p^1)u_N(r_1^1) + p^1 u_N(r_3^1) - u_N(r_2^1)) \le 0\},$$

where $h_1 = 1$ if $Z_1^1 \preceq Z_2^1$ and $h_1 = -1$ otherwise. We consider three cases.

(i) No information about the shape and the Lipschitz modulus. We obtain $p^1 = \ldots = p^{10} = 0.5$.

(ii) No information about the shape but with complete information about the Lipschitz modulus $L = 2$ of u^*. $p^1 = p^2 = p^3 = 0.5$, $p^4 = 0.35374$, $p^5 = 0.62686$, $p^6 = p^7 = 0.5$, $p^8 = 0.31244$, $p^9 = 0.34520$ and $p^{10} = 0.5$.

(iii) No information about Lipschitz modulus but with complete information about the S-shape with an inflection point 0. We obtain $p^1 = 0.33849$, $p^2 = 0.50312$, $p^3 = 0.73959$, $p^4 = 0.19973$, $p^5 = 0.70754$, $p^6 = 0.25000$, $p^7 = 0.25000$, $p^8 = 0.30879$, $p^9 = 0.31161$ and $p^{10} = 0.25000$.
Then $\mathcal{U}_N^{10} = \left\{u_N \in \mathcal{U}_N : h_m((1-p^m)u_N(r_1^m) + p^m u_N(r_3^m) - u_N(r_2^m)) \le 0,\ m = 1, \ldots, 10\right\}$. Let

$$\bar{u}_i = \max_{u_N \in \mathcal{U}_N^{10}, u_N(-0.5)=0, u_N(0.5)=1} u_N(x_i) \quad \text{and} \quad \underline{u}_i = \min_{u_N \in \mathcal{U}_N^{10}, u_N(-0.5)=0, u_N(0.5)=1} u_N(x_i),\ x_i \in \mathcal{X}.$$

Figure EC.2 (A1) depicts the curve passing through $\{(x_i, u_N(x_i))\}_{i=1}^N$ and the "**upper curve**" passing through $\{(x_i, \bar{u}_i)\}_{i=1}^N$, the "**lower curve**" through $\{(x_i, \underline{u}_i)\}_{i=1}^N$ in case (i). Figure EC.2 (A2) shows the lower and upper curves in case (ii). Figure EC.2 (A3) depicts the lower and upper curves in case (iii).

2. **Modified Polyhedral Method with No Information about the Shape and the Lipschitz Modulus**. Let us develop the modified polyhedral method for the utility function under the von Neumann and Morgenstern EUT. We begin with an initial polyhedron for the vector of increments of the utility function: $\Delta_0^{\mathrm{u}} := \{\boldsymbol{v} \in \mathbb{R}^{J_0^{\mathrm{u}}-2} : \boldsymbol{v} \ge 0, \boldsymbol{e}^\top \boldsymbol{v} \le 1\}$, where $\mathcal{X}_0^{\mathrm{u}} = \{-0.5, 0, 0.5, r_1^k, r_2^k, r_3^k : k = 1, 2, 3\}$ is the set of breakpoints of utility functions, where $\{(r_1^k, r_2^k, r_3^k)\}_{k=1}^3$ are obtained from the first three RRUS queries. Let $J_0^{\mathrm{u}} := |\mathcal{X}_0^{\mathrm{u}}| = 12$. We generate questionnaires based on the preference function $\mathbb{E}[u(\cdot)]$. In Steps 1–2, let $\boldsymbol{c}^m$ be the analytic center of $\Delta_{m-1}^{\mathrm{u}}$ and $\boldsymbol{v}_1^m$ and $\boldsymbol{v}_2^m$ be the two intersection points between the longest axis of Sonnevend's inner ellipsoid of the polyhedron $\Delta_{m-1}^{\mathrm{u}}$ and the boundary of the polyhedron. In Step 3, we generate the m-th pair of queries by solving the following two programs:

$$r_2^{m,i} \in \arg\max_x \left\{\rho_1(x; \boldsymbol{v}_1^m) : x \in [\underline{x}, \bar{x}],\ \rho_1(x; \boldsymbol{c}^m) \le D_i\right\}, \tag{EC.15a}$$

$$(r_1^{m,i}, r_3^{m,i}, p^{m,i}) \in \arg\max_{(x,y,p)} \left\{\rho_2((x,y,p); \boldsymbol{v}_2^m) : \begin{array}{l} x \in [\underline{x}, 0),\ y \in (0, \bar{x}],\ p \in (0,1) \\ \rho_2((x,y,p); \boldsymbol{c}^m) \le D_i \end{array}\right\}, \tag{EC.15b}$$

where $D_i \in \{\sum_{j=1}^i c_j^m : i = 1, \ldots, J_{m-1}^{\mathrm{u}} - 2\}$, $\rho_1(x; \boldsymbol{v}) = (\boldsymbol{R}\boldsymbol{v})^\top \boldsymbol{h}^{\mathcal{X}_{m-1}^{\mathrm{u}}}(x)$ and $\rho_2((x,y,p); \boldsymbol{v}) = (\boldsymbol{R}\boldsymbol{v})^\top((1-p)\boldsymbol{h}^{\mathcal{X}_{m-1}^{\mathrm{u}}}(x) + p\boldsymbol{h}^{\mathcal{X}_{m-1}^{\mathrm{u}}}(y))$. Note that in the formulations Z_2^m is uniquely determined by r_2^m and Z_1^m is uniquely determined by (r_1^m, r_3^m, p^m).

We select $(r_1^m, r_2^m, r_3^m) := (r_1^{m,s_0}, r_2^{m,s_0}, r_3^{m,s_0})$ from $\{(r_1^{m,i}, r_2^{m,i}, r_3^{m,i})\}_{i=1}^{J_{m-1}^{\mathrm{u}}-2}$ and set $p^m := p^{m,s_0}$, where $s_0 \in \arg\min_{s\in\{1,\ldots,J_{m-1}^{\mathrm{u}}-2\}} \left|(\boldsymbol{R}\boldsymbol{c}^m)^\top \left((1-p^{m,s})\boldsymbol{h}^{\mathcal{X}_{m-1}^{\mathrm{u}}}(r_1^{m,s}) + p^{m,s}\boldsymbol{h}^{\mathcal{X}_{m-1}^{\mathrm{u}}}(r_3^{m,s}) - \boldsymbol{h}^{\mathcal{X}_{m-1}^{\mathrm{u}}}(r_2^{m,s})\right)\right|$. This selects the cut hyperplane whose deviation from the analytic center is minimal. We then update the set of breakpoints: $\mathcal{X}_m^{\mathrm{u}} := \mathcal{X}_{m-1}^{\mathrm{u}} \cup \{r_1^m, r_3^m\}$ and $J_m^{\mathrm{u}} := |\mathcal{X}_m^{\mathrm{u}}|$ (see Zhang et al. 2025 for a more flexible polyhedral method). The ambiguity set of the utility functions is then constructed by

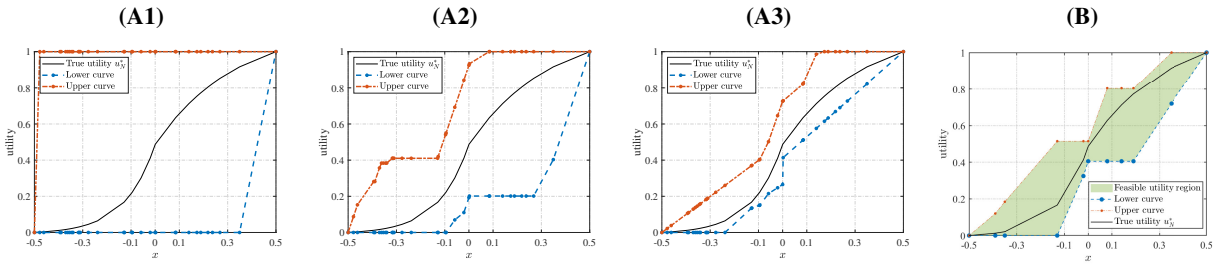
$$\mathcal{U}_m = \left\{u_{J_m^{\mathrm{u}}} : [\underline{x}, \bar{x}] \to [0,1] : h_l(\mathbb{E}[u_{J_m^{\mathrm{u}}}(Z_1^l)] - \mathbb{E}[u_{J_m^{\mathrm{u}}}(Z_2^l)]) \le 0,\ \forall l \in [m]\right\},$$

where $h_l = 1$ if $\mathbb{E}[u(Z_1^l)] \le \mathbb{E}[u(Z_2^l)]$, and $h_l = -1$ otherwise.

Figure EC.2 (B) depicts the results of the modified polyhedral method for eliciting the true utility function using 10 queries. We emphasize that the polyhedral method is more efficient for utility functions with no prior information on their shape or Lipschitz modulus.

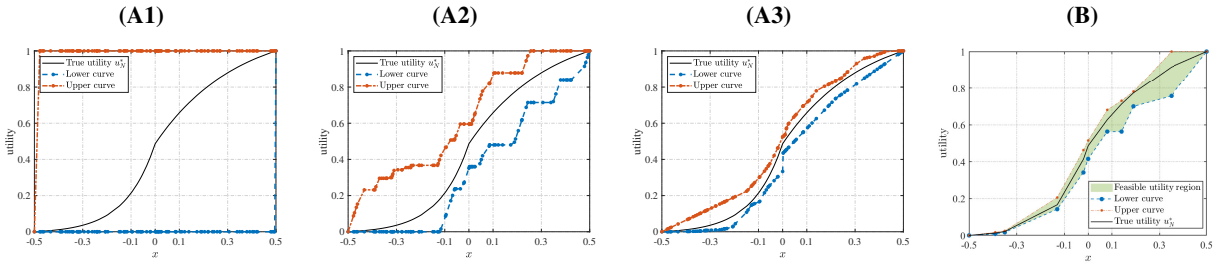
Moreover, we can generate $M \in \{30, 50, 100\}$ queries with parameters (r_1^m, r_2^m, r_3^m) with $m = 1, \ldots, M$. We then determine parameters p^m by random relative utility split scheme. Figures EC.3–EC.5 display the performances of utility function elicitation and the upper and lower curves generated by the resulting feasible set $\mathcal{U}_M$ with $J_M^{\mathrm{u}} = 3M + 3$. We can see that the modified polyhedral method performs much better than RRUS in all of the cases.

Figure EC.2 Ranges of Utility Functions under the RRUS Scheme and the Polyhedral Method



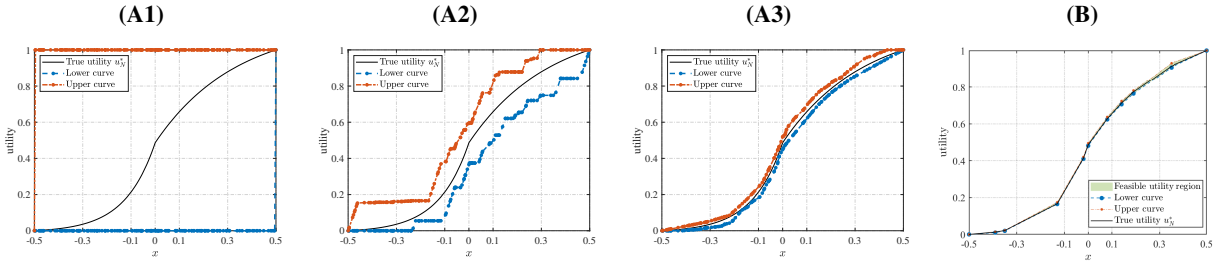
Note. **(A)** RRUS scheme for preference elicitation in the S-shaped utility setting with the range of utility functions $\mathcal{U}_N^M$ for $M = 10$. (A1) Case (i): no shape information and no Lipschitz constant L. The domain of the utility function is $[-0.5, 0.5]$ (x-axis). The vertical axis marks the range of the utility functions ($[0,1]$). The blue curve corresponds to $\{(x_i, \underline{u}_i)\}_{i=1}^N$. The orange curve corresponds to $\{(x_i, \bar{u}_i)\}_{i=1}^N$. (A2) Case (ii): with Lipschitz constant L but without the S-shape condition. (A3) Case (iii): with the S-shape condition but without Lipschitz constant L. **(B)** Polyhedral method for preference elicitation in the S-shaped utility setting with the range of utility functions $\mathcal{U}_M$ for $M = 10$ without prior information.

Figure EC.3 Ranges of Utility Functions under the RRUS Scheme and the Polyhedral Method for $M = 30$



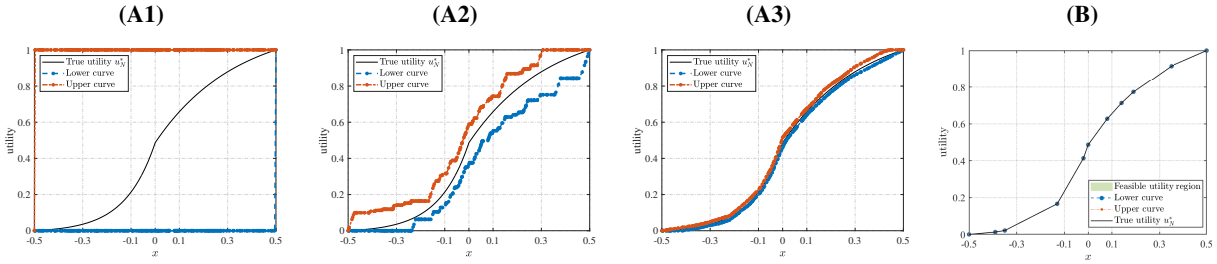
Note. **(A)** RRUS scheme for preference elicitation in the S-shaped utility setting with the range of utility functions $\mathcal{U}_N^M$ for $M = 30$. **(B)** Polyhedral method for preference elicitation in the S-shaped utility setting with the range of utility functions $\mathcal{U}_M$ for $M = 30$ without prior information. The labels, graphs and lines have the same interpretation as in Figure EC.2.

Figure EC.4 Ranges of Utility Functions under the RRUS Scheme and the Polyhedral Method for $M = 50$



Note. **(A)** RRUS scheme for preference elicitation in the S-shaped utility setting with the range of utility functions $\mathcal{U}_N^M$ for $M = 50$. **(B)** Polyhedral method for preference elicitation in the S-shaped utility setting with the range of utility functions $\mathcal{U}_M$ for $M = 50$ without prior information. The labels, graphs and lines have the same interpretation as in Figure EC.2.

Figure EC.5 Ranges of Utility Functions under the RRUS Scheme and the Polyhedral Method for $M = 100$



Note. **(A)** RRUS scheme for preference elicitation in the S-shaped utility setting with the range of utility functions $\mathcal{U}_N^M$ for $M = 100$. **(B)** Polyhedral method for preference elicitation in the S-shaped utility setting with the range of utility functions $\mathcal{U}_M$ for $M = 100$ without prior information. The labels, graphs and lines have the same interpretation as in Figure EC.2.

EC.15. Proof of Proposition 6

Proof of Proposition 6. Analogous to the arguments in the proof of Proposition 5, we have $\boldsymbol{c}^m = (\boldsymbol{c}_1^m, \boldsymbol{c}_2^m)$ with $\boldsymbol{R}\boldsymbol{c}_1^m > 0$ and $\boldsymbol{R}\boldsymbol{c}_2^m > 0$. By the assumption that $\widetilde{\boldsymbol{\sigma}}_2^{1m}$ and $\widetilde{\boldsymbol{v}}_+^{2m}$ have no zero

components, it follows that $p^{m,i}$ and $r_{2+}^{m,i}$ satisfy

$$\begin{bmatrix} \boldsymbol{R}\boldsymbol{c}_1^m \\ \boldsymbol{R}\boldsymbol{c}_2^m \end{bmatrix}^\top \begin{bmatrix} 0 \\ \boldsymbol{h}^{\mathcal{S}_2}(p^{m,i}) \end{bmatrix} = D_i \quad \text{and} \quad \begin{bmatrix} \boldsymbol{R}\boldsymbol{c}_1^m \\ \boldsymbol{R}\boldsymbol{c}_2^m \end{bmatrix}^\top \begin{bmatrix} \boldsymbol{h}^{\mathcal{X}_+^{m-1}}(r_{2+}^{m,i}) \\ 0 \end{bmatrix} = D_i$$

for $i \in [N_2-2]$. Then $l_{\text{cut},+}^{m,m-1}(\boldsymbol{c}^m) = h_m((\boldsymbol{R}\boldsymbol{c}_2^m)^\top \boldsymbol{h}^{\mathcal{S}_2}(p^{m,i}) - (\boldsymbol{R}\boldsymbol{c}_1^m)^\top \boldsymbol{h}^{\mathcal{X}_+^{m-1}}(r_{2+}^{m,i})) = h_m(D_i - D_i) = 0$ for $i \in [N_2-2]$. Hence the cut hyperplane $l_{\text{cut},+}^{m,m-1}(\cdot)$ passes through the analytic center $\boldsymbol{c}^m$. The proof is complete. □

EC.16. Proof of Proposition 7

Proof of Proposition 7. Recall that the analytic center of the polyhedron that is defined by a set of linear inequalities $\tilde{\boldsymbol{a}}_i^\top \boldsymbol{x} \le \tilde{b}_i$, $i \in [I]$ is defined as an optimal solution of the problem:

$$\min_{\boldsymbol{x}} \; -\sum_{i=1}^{I} \log(\tilde{b}_i - \tilde{\boldsymbol{a}}_i^\top \boldsymbol{x}).$$

If we assume that $\|\tilde{\boldsymbol{a}}_i\| = 1$, for $i \in [I]$, then the slack

$$\tilde{b}_i - \tilde{\boldsymbol{a}}_i^\top \boldsymbol{x} = \text{the distance of } \boldsymbol{x} \text{ to the hyperplane } \mathcal{H}_i = \{\boldsymbol{x} : \tilde{\boldsymbol{a}}_i^\top \boldsymbol{x} = \tilde{b}_i\}.$$

The analytic center is the point that maximizes the product of distances to the defining hyperplanes $\tilde{\boldsymbol{a}}_i^\top \boldsymbol{x} = \tilde{b}_i$, for $i \in [I]$ (see Boyd and Vandenberghe 2004, p. 420). For the case of Δ_+^m, to ease the exposition, we set the updated initial set $\Delta_+^0 = \{(\widetilde{\boldsymbol{v}}_+, \widetilde{\boldsymbol{\sigma}}_2) \in \mathbb{R}^{J_+ + N_2 - 4} : \boldsymbol{A}(\widetilde{\boldsymbol{v}}_+, \widetilde{\boldsymbol{\sigma}}_2) \le \boldsymbol{b}\}$, where $\boldsymbol{A} \in \mathbb{R}^{(2J_+ + N_2 - 4) \times (J_+ + N_2 - 4)}$ and $\boldsymbol{b} \in \mathbb{R}^{2J_+ + N_2 - 4}$. The analytic center $\boldsymbol{c}_+^m$ of polyhedron Δ_+^{m-1} is the optimal solution of the following problem w.r.t. $(\widetilde{\boldsymbol{v}}_+, \widetilde{\boldsymbol{\sigma}}_2)$:

$$\begin{aligned} \max_{\widetilde{\boldsymbol{v}}_+, \widetilde{\boldsymbol{\sigma}}_2, \boldsymbol{s}} \quad & \sum_{i=1}^{2J_+^{m-1} + N_2 - 4 + m - 1} \log(s_i) \\ \text{s.t.} \quad & \boldsymbol{A}(\widetilde{\boldsymbol{v}}_+, \widetilde{\boldsymbol{\sigma}}_2) + \boldsymbol{s}_{[2J_+^{m-1} + N_2 - 4]} = \boldsymbol{b}, \; \boldsymbol{s} \ge 0, \\ & h_l\big((\boldsymbol{R}\widetilde{\boldsymbol{\sigma}}_2)^\top \boldsymbol{h}^{\mathcal{S}_2}(p^l) - (\boldsymbol{R}\widetilde{\boldsymbol{v}}_+)^\top \boldsymbol{h}^{\mathcal{X}_+^{m-1}}(r_{2+}^l)\big) + s_{2J_+^{m-1} + N_2 - 4 + l} = 0, \; \forall l \in [m-1], \end{aligned}$$

where $\boldsymbol{s}_{[2J_+^{m-1} + N_2 - 4]} = (s_1, \cdots, s_{2J_+^{m-1} + N_2 - 4})$ and $\boldsymbol{s} := (s_1, \cdots, s_{2J_+^{m-1} + N_2 - 4 + m - 1}) \in \mathbb{R}^{2J_+^{m-1} + N_2 - 4 + m - 1}$. For the ambiguity set Δ_+^{m-2}, the analytic center, denoted by $\boldsymbol{c}_+^{m-1}$, maximizes

$$\begin{aligned} \vartheta_{m-1}(\widetilde{\boldsymbol{v}}_+, \widetilde{\boldsymbol{\sigma}}_2) := & \sum_{j=1}^{2J_+^{m-2} + N_2 - 4} \log(b_j - \boldsymbol{a}_j^\top(\widetilde{\boldsymbol{v}}_+, \widetilde{\boldsymbol{\sigma}}_2)) \\ & + \sum_{l=1}^{m-2} \log\Big(- h_l\big((\boldsymbol{R}\widetilde{\boldsymbol{\sigma}}_2)^\top \boldsymbol{h}^{\mathcal{S}_2}(p^l) - (\boldsymbol{R}\widetilde{\boldsymbol{v}}_+)^\top \boldsymbol{h}^{\mathcal{X}_+^{m-2}}(r_{2+}^l)\big)\Big). \end{aligned}$$

For the ambiguity set Δ_+^{m-1} with $\mathcal{X}_+^{m-1} = \mathcal{X}_+^{m-2}$, the analytic center $\boldsymbol{c}_+^m$ maximizes

$$\begin{aligned}\vartheta_m(\widetilde{\boldsymbol{v}}_+, \widetilde{\boldsymbol{\sigma}}_2) = &\sum_{j=1}^{2J_+^{m-1}+N_2-4} \log(b_j - \boldsymbol{a}_j^\top(\widetilde{\boldsymbol{v}}_+, \widetilde{\boldsymbol{\sigma}}_2)) \\ &+ \sum_{l=1}^{m-1} \log\Big(- h_l\big((\boldsymbol{R}\widetilde{\boldsymbol{\sigma}}_2)^\top \boldsymbol{h}^{\mathcal{S}_2}(p^l) - (\boldsymbol{R}\widetilde{\boldsymbol{v}}_+)^\top \boldsymbol{h}^{\mathcal{X}_+^{m-1}}(r_{2+}^l)\big)\Big) \\ :=&\vartheta_{m-1}(\widetilde{\boldsymbol{v}}_+, \widetilde{\boldsymbol{\sigma}}_2) + \log\Big(- h_{m-1}\big((\boldsymbol{R}\widetilde{\boldsymbol{\sigma}}_2)^\top \boldsymbol{h}^{\mathcal{S}_2}(p^{m-1}) - (\boldsymbol{R}\widetilde{\boldsymbol{v}}_+)^\top \boldsymbol{h}^{\mathcal{X}_+^{m-1}}(r_{2+}^{m-1})\big)\Big).\end{aligned}$$

Note that $\boldsymbol{c}_+^m \in \Delta_+^{m-1}$, $\boldsymbol{c}_+^{m-1} \in \Delta_+^{m-2}$ make the objective functions $\vartheta_m(\widetilde{\boldsymbol{v}}_+, \widetilde{\boldsymbol{\sigma}}_2)$ and $\vartheta_{m-1}(\widetilde{\boldsymbol{v}}_+, \widetilde{\boldsymbol{\sigma}}_2)$ attain the optimal values, respectively.

By the fact that $\delta_{m-1} := -h_{m-1}\big((\boldsymbol{R}\boldsymbol{c}_2^m)^\top \boldsymbol{h}^{\mathcal{S}_2}(p^{m-1}) - (\boldsymbol{R}\boldsymbol{c}_1^m)^\top \boldsymbol{h}^{\mathcal{X}_+^{m-1}}(r_{2+}^{m-1})\big) \in (0,1)$ with $\boldsymbol{c}_+^m = (\boldsymbol{c}_1^m, \boldsymbol{c}_2^m)$, we have $\log(\delta_{m-1}) < 0$ and subsequently,

$$\vartheta_m(\boldsymbol{c}_+^m) < \vartheta_{m-1}(\boldsymbol{c}_+^m) \le \vartheta_{m-1}(\boldsymbol{c}_+^{m-1}).$$

Note that the above inequality still holds when the vector $\boldsymbol{a}_i$ for $i \in [2J_+^{m-1} + N_2 - 4]$ of matrix $\boldsymbol{A}$ and the coefficient vector of $-h_l\big((\boldsymbol{R}\widetilde{\boldsymbol{\sigma}}_2)^\top \boldsymbol{h}^{\mathcal{S}_2}(p^l) - (\boldsymbol{R}\widetilde{\boldsymbol{v}}_+)^\top \boldsymbol{h}^{\mathcal{X}_+^{m-2}}(r_{2+}^l)\big)$, for $l \in [m-1]$, are normalized. By construction, $\Delta_+^{m-1} \subseteq \Delta_+^{m-2}$, so the feasible region shrinks as the number of queries increases. The proof is complete. □

EC.17. An Example of the Modified Polyhedral Method

In this section, we present an example of the modified polyhedral method introduced in Section 4.2.1.

Example EC.5 (Illustration of the Polyhedral Method for $\widehat{g}_2$). We use a simple example to explain the steps in the polyhedral method, where the true utility function is $v_+^*(x) = (1 - e^{-3x})/3$ for $x > 0$ defined over $[0, 0.5]$ and the true distortion function is $g_2^*(t) = t^\gamma/(t^\gamma + (1-t)^\gamma)$ for $\gamma = 0.6$ defined over $[0, 1]$. The piecewise linear value function has three breakpoints, i.e., $J_+ = 3$ including the two ends of the interval and the one within it is 0.25, that is, $x_1 = 0$, $x_2 = 0.25$, $x_3 = 0.5$. The piecewise linear distortion function has four breakpoints, i.e., $N_2 = 4$ including the two ends of $[0, 1]$ and the two interior breakpoints are 0.3 and 0.6, that is, $t_1 = 0$, $t_2 = 0.3$, $t_3 = 0.6$, $t_4 = 1$. Consider the normalized value function on $[0, 0.5]$. The true increment vectors of the value function and the distortion function are given by $\boldsymbol{v}_+^* = (0.679, 0.321)$, $\boldsymbol{\sigma}_2^* = (0.376, 0.185, 0.439)$, and $(\widetilde{\boldsymbol{v}}_+^*, \widetilde{\boldsymbol{\sigma}}_2^*) = (v_{+,1}, \sigma_{2,1}, \sigma_{2,2}) = (0.679, 0.376, 0.185)$ (these are all column vectors: we write them in row format in running text). We impose the concavity of the value function v_+. To ease the exposition, we do not update the set of breakpoints of the value function. The parameter D_i

in (35) is set to a randomly generated constant D. The l-th cutting hyperplane is constructed as $\tilde{\boldsymbol{\sigma}}_2^\top \boldsymbol{h}^{\mathcal{S}_2}_{[N_2-1]}(p^l) - \tilde{\boldsymbol{v}}_+^\top \boldsymbol{h}^{\mathcal{X}_+}_{[J_+-1]}(r^l_{2+})$, where $\mathcal{S}_2 = \{t_1, t_2, t_3, t_4\}$, $\mathcal{X}_+ = \{x_1, x_2, x_3\}$, $\boldsymbol{h}^{\mathcal{S}_2}_{[N_2-1]}(p^l)$ and $\boldsymbol{h}^{\mathcal{X}_+}_{[J_+-1]}(r^l_{2+})$ denote the truncated vectors consisting of the first N_2-1 and J_+-1 entries. We focus on the iteration of the polyhedral method.

$$\Delta_+^0 = \{(v_{+,1}, \sigma_{2,1}, \sigma_{2,2}) \in \mathbb{R}^{1+2} : v_{+,1} \le 1,\ v_{+,1} \ge 0,\ \sigma_{2,1} + \sigma_{2,2} \le 1,\ \sigma_{2,i} \ge 0, i = 1, 2\}.$$

Iteration 1. **Step 1**: The analytic center of Δ_+^0 is $\boldsymbol{c}^1 = (0.789, 0.333, 0.333)$. **Step 2**: $(v_{+,1}^{11}, \sigma_{2,1}^{11}, \sigma_{2,2}^{11}) = (0.789, 0.667, 0)$, $(v_{+,1}^{21}, \sigma_{2,1}^{21}, \sigma_{2,2}^{21}) = (0.789, 0, 0.667)$. **Step 3**: $p^1 = 0.9496$, $r^1_{2+} = 0.4503$ ($D = 0.958$). Then the cutting hyperplane is $-v_{+,1} + \sigma_{2,1} + \sigma_{2,2} = 0$, $h_1 = 1$. The 1st polyhedron is

$$\Delta_+^1 = \Delta_+^0 \cap \{(v_{+,1}, \sigma_{2,1}, \sigma_{2,2}) \in \mathbb{R}^{1+2} : -v_{+,1} + \sigma_{2,1} + \sigma_{2,2} \le 0\}.$$

Iteration 2. **Step 1**: The analytic center of Δ_+^1 is $\boldsymbol{c}^2 = (0.848, 0.228, 0.228)$. **Step 2**: $(v_{+,1}^{12}, \sigma_{2,1}^{12}, \sigma_{2,2}^{12}) = (0.848, 0.456, 0)$, $(v_{+,1}^{22}, \sigma_{2,1}^{22}, \sigma_{2,2}^{22}) = (0.848, 0, 0.456)$. **Step 3**: $p^2 = 0.6030$, $r^2_{2+} = 0.1355$ ($D = 0.46$). Then the cutting hyperplane is $-0.542 v_{+,1} + \sigma_{2,1} + \sigma_{2,2} = 0$, $h_2 = -1$. The 2nd polyhedron is

$$\Delta_+^2 = \Delta_+^1 \cap \{(v_{+,1}, \sigma_{2,1}, \sigma_{2,2}) \in \mathbb{R}^{1+2} : -0.542 v_{+,1} + \sigma_{2,1} + \sigma_{2,2} \ge 0\}.$$

Iteration 3. **Step 1**: The analytic center of Δ_+^2 is $\boldsymbol{c}^3 = (0.847, 0.328, 0.328)$. **Step 2**: $(v_{+,1}^{13}, \sigma_{2,1}^{13}, \sigma_{2,2}^{13}) = (0.847, 0.656, 0)$, $(v_{+,1}^{23}, \sigma_{2,1}^{23}, \sigma_{2,2}^{23}) = (0.847, 0, 0.656)$. **Step 3**: $p^3 = 0.6049$, $r^3_{2+} = 0.1948$ ($D = 0.66$). Then the cutting hyperplane is $-0.779 v_{+,1} + \sigma_{2,1} + \sigma_{2,2} = 0$, $h_3 = 1$. The 3rd polyhedron is

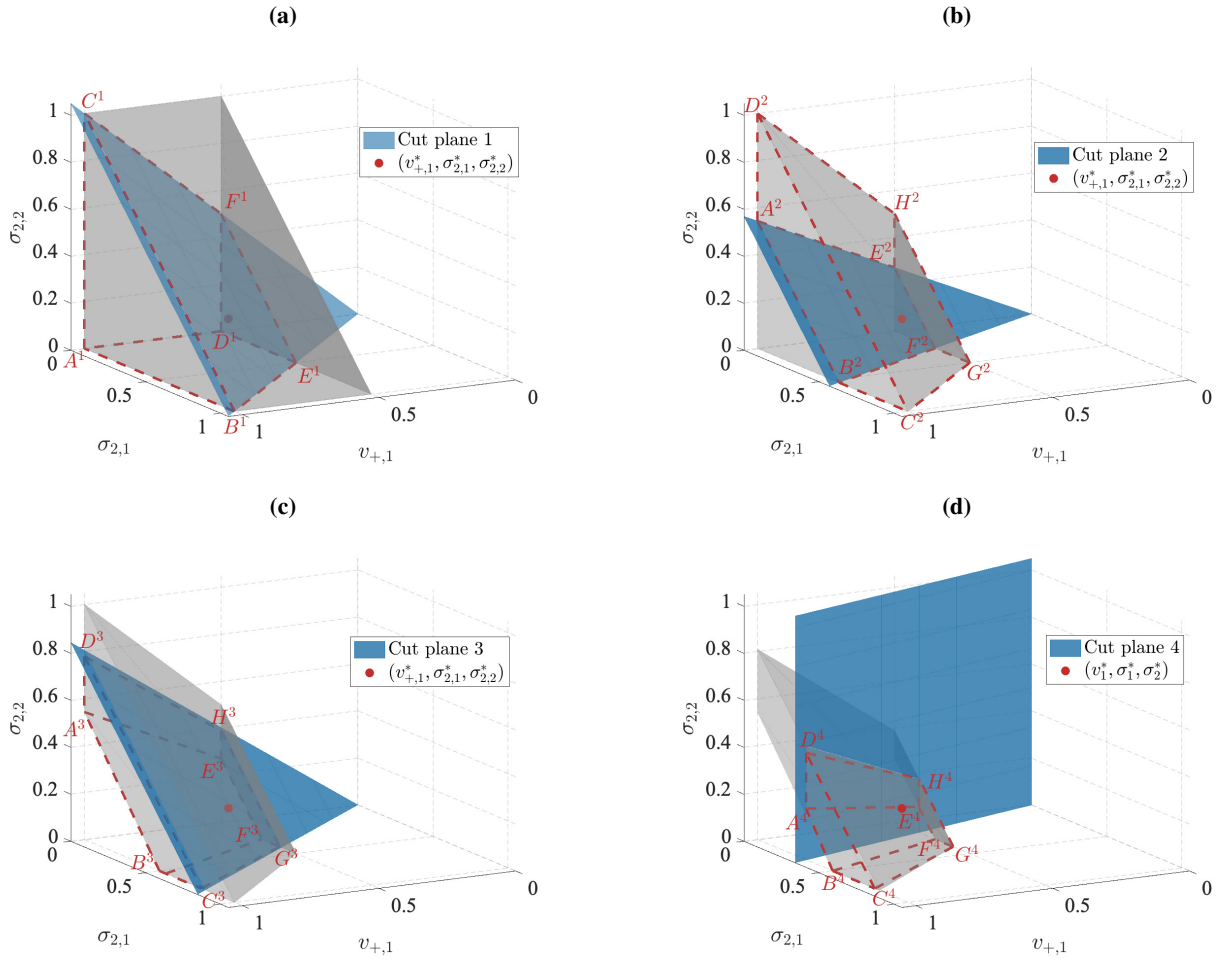
$$\Delta_+^3 = \Delta_+^2 \cap \{(v_{+,1}, \sigma_{2,1}, \sigma_{2,2}) \in \mathbb{R}^{1+2} : -0.779 v_{+,1} + \sigma_{2,1} + \sigma_{2,2} \le 0\}.$$

Iteration 4. **Step 1**: The analytic center of Δ_+^3 is $\boldsymbol{c}^4 = (0.875, 0.284, 0.284)$. **Step 2**: $(v_{+,1}^{14}, \sigma_{2,1}^{14}, \sigma_{2,2}^{14}) = (0.875, 0.567, 0)$, $(v_{+,1}^{24}, \sigma_{2,1}^{24}, \sigma_{2,2}^{24}) = (0.875, 0, 0.567)$. **Step 3**: $p^4 = 0.1903$, $r^4_{2+} = 0.0514$ ($D = 0.18$). Then the cutting hyperplane is $-0.205 v_{+,1} + 0.634 \sigma_{2,1} = 0$, $h_4 = -1$. The 4th polyhedron is

$$\Delta_+^4 = \Delta_+^3 \cap \{(v_{+,1}, \sigma_{2,1}, \sigma_{2,2}) \in \mathbb{R}^{1+2} : -0.206 v_{+,1} + 0.634 \sigma_{2,1} \ge 0\}.$$

The cutting hyperplanes and the polyhedra Δ_+^i for $i = 1, 2, 3, 4$ are presented in Figure EC.6.

Figure EC.6 Visualization of the cut planes and the resulting polyhedron Δ_+^m for $m = 1, 2, 3, 4$.



Note. The red point is $(v_{+,1}^*, \sigma_{2,1}^*, \sigma_{2,2}^*) = (0.679, 0.375, 0.185)$. **(a)** The grey polyhedron represents Δ_+^0 and the one framed by the red dashed lines is Δ_+^1 (A^1-B^1-C^1-D^1-E^1-F^1) after the first cut. The cut plane is $-v_{+,1} + \sigma_{2,1} + \sigma_{2,2} = 0$. $h_1 = 1$. **(b)** The resulting polyhedron Δ_+^2: A^2-B^2-C^2-D^2-E^2-F^2-G^2-H^2 corresponding to $h_2 = -1$. **(c)** The resulting polyhedron Δ_+^3: A^3-B^3-C^3-D^3-E^3-F^3-G^3-H^3 corresponding to $h_3 = 1$. **(d)** The resulting polyhedron Δ_+^4: A^4-B^4-C^4-D^4-E^4-F^4-G^4-H^4 corresponding to $h_4 = -1$.

EC.18. Piecewise McCormick Relaxation: Implementation Details

In this section, we present a piecewise linearization of the bilinear terms $v_{+,i}\sigma_{2,j}$ and $v_{-,i}\sigma_{1,j}$ appearing in the objective function (54a).

Piecewise Linearization of Bilinear Term $v_{+,i}\sigma_{2,j}$. For each $j \in [N_2 - 1]$, we divide the domain $[\sigma_{2,j}^L, \sigma_{2,j}^U]$ of $\sigma_{2,j}$ into N equally sized, mutually exclusive sub-regions. Next, we calculate the lower and upper bounds of $\sigma_{2,j}$ in each sub-region:

$$\sigma_{2,j,n}^L := \sigma_{2,j}^L + \frac{(\sigma_{2,j}^U - \sigma_{2,j}^L)(n-1)}{N} \quad \text{and} \quad \sigma_{2,j,n}^U := \sigma_{2,j}^L + \frac{(\sigma_{2,j}^U - \sigma_{2,j}^L)n}{N}, \; n \in [N]. \tag{EC.16}$$

Let $\boldsymbol{\sigma}_{2,j}^L := (\sigma_{2,j,1}^L, \cdots, \sigma_{2,j,N}^L)$ and $\boldsymbol{\sigma}_{2,j}^U := (\sigma_{2,j,1}^U, \cdots, \sigma_{2,j,N}^U)$, for $j \in [N_2 - 1]$. In the piecewise McCormick relaxation, we define $w_{ij}^+ := v_{+,i}\sigma_{2,j}$, for $i \in [J_+^{M_2} - 1]$ and $j \in [N_2 - 1]$. By introducing

binary variables $\boldsymbol{y}_j^{g_2} = (y_{j,1}^{g_2}, \cdots, y_{j,N}^{g_2})$ to represent that $\sigma_{2,j}$ lies within sub-region $[\sigma_{2,j,n}^L, \sigma_{2,j,n}^U]$ or not, we have

$$w_{ij}^+ \geq v_{+,i}^L \sigma_{2,j} + ((\boldsymbol{\sigma}_{2,j}^L)^\top \boldsymbol{y}_j^{g_2}) v_{+,i} - v_{+,i}^L ((\boldsymbol{\sigma}_{2,j}^L)^\top \boldsymbol{y}_j^{g_2}), \tag{EC.17a}$$

$$w_{ij}^+ \geq v_{+,i}^U \sigma_{2,j} + ((\boldsymbol{\sigma}_{2,j}^U)^\top \boldsymbol{y}_j^{g_2}) v_{+,i} - v_{+,i}^U ((\boldsymbol{\sigma}_{2,j}^U)^\top \boldsymbol{y}_j^{g_2}), \tag{EC.17b}$$

$$w_{ij}^+ \leq v_{+,i}^U \sigma_{2,j} + ((\boldsymbol{\sigma}_{2,j}^L)^\top \boldsymbol{y}_j^{g_2}) v_{+,i} - v_{+,i}^U ((\boldsymbol{\sigma}_{2,j}^L)^\top \boldsymbol{y}_j^{g_2}), \tag{EC.17c}$$

$$w_{ij}^+ \leq v_{+,i}^L \sigma_{2,j} + ((\boldsymbol{\sigma}_{2,j}^U)^\top \boldsymbol{y}_j^{g_2}) v_{+,i} - v_{+,i}^L ((\boldsymbol{\sigma}_{2,j}^U)^\top \boldsymbol{y}_j^{g_2}), \tag{EC.17d}$$

$$\boldsymbol{e}^\top \boldsymbol{y}_j^{g_2} = 1, \tag{EC.17e}$$

where $\boldsymbol{y}_j^{g_2}, \boldsymbol{\sigma}_{2,j}^L, \boldsymbol{\sigma}_{2,j}^U \in \mathbb{R}^N$ for $j \in [N_2 - 1]$, and constraint (EC.17e) ensures that $\sigma_{2,j}$ lies within a single sub-region. There are bilinear terms $y_{j,n}^{g_2} v_{+,i}$ in constraints (EC.17a)–(EC.17d). Furthermore, we apply the McCormick relaxation to each bilinear term $y_{j,n}^{g_2} v_{+,i}$. Specifically, let $\widehat{V}_{j,n,i}^+ := y_{j,n}^{g_2} v_{+,i}$, where $y_{j,n}^{g_2} \in \{0,1\}$, $(\boldsymbol{\sigma}_{2,j}^L)^\top \boldsymbol{y}_j^{g_2} \leq \sigma_{2,j} \leq (\boldsymbol{\sigma}_{2,j}^U)^\top \boldsymbol{y}_j^{g_2}$, for $i \in [J_+^{M_2} - 1]$, $j \in [N_2 - 1]$, $n \in [N]$. Then

$$\widehat{V}_{j,n,i}^+ \geq y_{j,n}^{g_2} v_{+,i}^L, \ \widehat{V}_{j,n,i}^+ \geq v_{+,i} + y_{j,n}^{g_2} v_{+,i}^U - v_{+,i}^U, \ \widehat{V}_{j,n,i}^+ \leq v_{+,i} + y_{j,n}^{g_2} v_{+,i}^L - v_{+,i}^L, \ \widehat{V}_{j,n,i}^+ \leq y_{j,n}^{g_2} v_{+,i}^U, \tag{EC.18}$$

for $i \in [J_+^{M_2} - 1]$, $j \in [N_2 - 1]$, $n \in [N]$. Consequently, by introducing $\sigma_{2,j,n}^L$ and $\sigma_{2,j,n}^U$ from (EC.16) along with the definition $\widehat{V}_{j,n,i}^+ = y_{j,n}^{g_2} v_{+,i}$, we can reformulate the inequality system (EC.17) as

$$w_{ij}^+ \geq v_{+,i}^L \sigma_{2,j} + \sum_{n=1}^N \left(\sigma_{2,j,n}^L \widehat{V}_{j,n,i}^+ \right) - v_{+,i}^L ((\boldsymbol{\sigma}_{2,j}^L)^\top \boldsymbol{y}_j^{g_2}), \tag{EC.19a}$$

$$w_{ij}^+ \geq v_{+,i}^U \sigma_{2,j} + \sum_{n=1}^N \left(\sigma_{2,j,n}^U \widehat{V}_{j,n,i}^+ \right) - v_{+,i}^U ((\boldsymbol{\sigma}_{2,j}^U)^\top \boldsymbol{y}_j^{g_2}), \tag{EC.19b}$$

$$w_{ij}^+ \leq v_{+,i}^U \sigma_{2,j} + \sum_{n=1}^N \left(\sigma_{2,j,n}^L \widehat{V}_{j,n,i}^+ \right) - v_{+,i}^U ((\boldsymbol{\sigma}_{2,j}^L)^\top \boldsymbol{y}_j^{g_2}), \tag{EC.19c}$$

$$w_{ij}^+ \leq v_{+,i}^L \sigma_{2,j} + \sum_{n=1}^N \left(\sigma_{2,j,n}^U \widehat{V}_{j,n,i}^+ \right) - v_{+,i}^L ((\boldsymbol{\sigma}_{2,j}^U)^\top \boldsymbol{y}_j^{g_2}), \tag{EC.19d}$$

$$(\boldsymbol{\sigma}_{2,j}^L)^\top \boldsymbol{y}_j^{g_2} \leq \sigma_{2,j} \leq (\boldsymbol{\sigma}_{2,j}^U)^\top \boldsymbol{y}_j^{g_2}, \ \forall j \in [N_2 - 1], \tag{EC.19e}$$

$$\boldsymbol{e}^\top \boldsymbol{y}_j^{g_2} = 1, \ \boldsymbol{y}_j^{g_2} \in \{0,1\}^N, \text{ constraints (EC.18)}. \tag{EC.19f}$$

In this way, we obtain a piecewise linear relaxation of the bilinear term $v_{+,i}\sigma_{2,j}$ in (EC.19) by using the piecewise McCormick relaxation.

Piecewise Linearization of the Bilinear Term $v_{-,i}\sigma_{1,j}$. Analogous to the discussions about $v_{+,i}\sigma_{2,j}$, we divide the range of each $\sigma_{1,j}$ into N sub-regions and then apply the McCormick relaxation to each sub-region. Specifically, for $\sigma_{1,j}$, $j \in [N_1 - 1]$, define $\sigma^L_{1,j,n}$ and $\sigma^U_{1,j,n}$ accordingly. Let $\boldsymbol{\sigma}^L_{1,j} := (\sigma^L_{1,j,1}, \ldots, \sigma^L_{1,j,N})$ and $\boldsymbol{\sigma}^U_{1,j} := (\sigma^U_{1,j,1}, \ldots, \sigma^U_{1,j,N})$. Let $w^-_{ij} := v_{-,i}\sigma_{1,j}$ for $i \in [J^{M_1}_- - 1]$ and $j \in [N_1 - 1]$ and introduce binary variables $\boldsymbol{y}^{g_1}_j := (y^{g_1}_{j,1}, \ldots, y^{g_1}_{j,N})$, for $j \in [N_1 - 1]$ to represent $\sigma_{1,j}$ which lies within sub-region $[\sigma^L_{1,j,n}, \sigma^U_{1,j,n}]$ or not. Next, we apply the McCormick relaxation to the bilinear term $y^{g_1}_{j,n} v_{-,i}$ over each sub-region. Denote $\widehat{V}^-_{j,n,i} := y^{g_1}_{j,n} v_{-,i}$ for $i \in [J^{M_1}_- - 1]$ and $j \in [N_1 - 1]$. Analogous to system (EC.19), we can develop constraints for $(\boldsymbol{w}^-, \boldsymbol{\sigma}_1, \widehat{\boldsymbol{V}}^-, \boldsymbol{y}^{g_1})$:

$$w^-_{ij} \geq v^L_{-,i}\sigma_{1,j} + \sum_{n=1}^{N} \left(\sigma^L_{1,j,n}\widehat{V}^-_{j,n,i}\right) - v^L_{-,i}((\boldsymbol{\sigma}^L_{1,j})^\top \boldsymbol{y}^{g_1}_j), \tag{EC.20a}$$

$$w^-_{ij} \geq v^U_{-,i}\sigma_{1,j} + \sum_{n=1}^{N} \left(\sigma^U_{1,j,n}\widehat{V}^-_{j,n,i}\right) - v^U_{-,i}((\boldsymbol{\sigma}^U_{1,j})^\top \boldsymbol{y}^{g_1}_j), \tag{EC.20b}$$

$$w^-_{ij} \leq v^U_{-,i}\sigma_{1,j} + \sum_{n=1}^{N} \left(\sigma^L_{1,j,n}\widehat{V}^-_{j,n,i}\right) - v^U_{-,i}((\boldsymbol{\sigma}^L_{1,j})^\top \boldsymbol{y}^{g_1}_j), \tag{EC.20c}$$

$$w^-_{ij} \leq v^L_{-,i}\sigma_{1,j} + \sum_{n=1}^{N} \left(\sigma^U_{1,j,n}\widehat{V}^-_{j,n,i}\right) - v^L_{-,i}((\boldsymbol{\sigma}^U_{1,j})^\top \boldsymbol{y}^{g_1}_j), \tag{EC.20d}$$

$$(\boldsymbol{\sigma}^L_{1,j})^\top \boldsymbol{y}^{g_1}_j \leq \sigma_{1,j} \leq (\boldsymbol{\sigma}^U_{1,j})^\top \boldsymbol{y}^{g_1}_j, \ \forall j \in [N_1 - 1], \tag{EC.20e}$$

$$\boldsymbol{e}^\top \boldsymbol{y}^{g_1}_j = 1, \ \boldsymbol{y}^{g_1}_j \in \{0,1\}^N, \tag{EC.20f}$$

$$\widehat{V}^-_{j,n,i} \geq y^{g_1}_{j,n} v^L_{-,i}, \ \widehat{V}^-_{j,n,i} \geq v_{-,i} + y^{g_1}_{j,n} v^U_{-,i} - v^U_{-,i}, \ \widehat{V}^-_{j,n,i} \leq v_{-,i} + y^{g_1}_{j,n} v^L_{-,i} - v^L_{-,i}, \ \widehat{V}^-_{j,n,i} \leq y^{g_1}_{j,n} v^U_{-,i}, \tag{EC.20g}$$

where $\sigma^L_{1,j,n} = \sigma^L_{1,j} + \frac{(\sigma^U_{1,j} - \sigma^L_{1,j})(n-1)}{N}$ and $\sigma^U_{1,j,n} = \sigma^L_{1,j} + \frac{(\sigma^U_{1,j} - \sigma^L_{1,j})n}{N}$ for $n \in [N]$. In this way, we obtain a piecewise linear relaxation of the bilinear term $v_{-,i}\sigma_{1,j}$ in (EC.20) by using piecewise McCormick relaxation.

EC.19. Remarks on the PRO Model $\rho_{\mathbb{V}\mathbb{G}_1\mathbb{G}_2}(f(\boldsymbol{z}, \boldsymbol{\zeta}))$ in Section 5

We apply the proposed robust shortfall risk measure to a multivariate decision-making problem with a loss function

$$\rho_{\mathbb{V}\mathbb{G}_1\mathbb{G}_2}(f(\boldsymbol{z}, \boldsymbol{\zeta})) := \inf_{x \in \mathbb{R}} \left\{ x : \sup_{(v, g_1, g_2) \in \mathbb{V}\mathbb{G}_1\mathbb{G}_2} \mathbb{E}_{g_1 g_2}[v(f(\boldsymbol{z}, \boldsymbol{\zeta}) - x)] \leq v(0) \right\},$$

where $z \in \mathbb{R}^n$ is a decision vector in the feasible set $Z \subset \mathbb{R}^n$, $\zeta : \Omega \to \mathbb{R}^n$ is a random vector, $f(z,\zeta) = z^\top \zeta$ represents a financial loss. In this case, we cannot directly apply the bisection method to solve this problem because we have to tackle z and x simultaneously and the constraint function is multivariate which is not necessarily monotonic w.r.t. (x,z). Let $\mathbb{V}_J\mathbb{G}_{1N_1}\mathbb{G}_{2N_2}$ be defined as in (25). We can use $\mathbb{V}_J\mathbb{G}_{1N_1}\mathbb{G}_{2N_2}$ to approximate the ambiguity set $\mathbb{V}\mathbb{G}_1\mathbb{G}_2$, and then consider the approximate preference robust problem:

$$\inf_{z\in Z} \rho_{\mathbb{V}_J\mathbb{G}_{1N_1}\mathbb{G}_{2N_2}}(f(z,\zeta)) := \inf_{x\in\mathbb{R}, z\in Z} \left\{ x : \sup_{(v,g_1,g_2)\in \mathbb{V}_J\mathbb{G}_{1N_1}\mathbb{G}_{2N_2}} \mathbb{E}_{g_1 g_2}[v(f(z,\zeta)-x)] \le v(0) \right\}. \tag{EC.21}$$

For any fixed (x,z), we order the scenarios so that $f(z,\zeta_1) \le \cdots \le f(z,\zeta_K)$, with the probabilities p_k reordered accordingly, and reformulate the inner maximization problem as follows:

$$\begin{aligned} \sup_{\nu_-,\nu_+,\sigma_1,\sigma_2} \Bigg\{ & \sum_{k=1}^{K_0(z,x)-1} \left((\nu_-)^\top \boldsymbol{h}^{\chi_-^{M_1}}(f(z,\zeta_k)-x)-1\right)\sigma_1^\top(\boldsymbol{h}^{\mathcal{S}_1}(q_k)-\boldsymbol{h}^{\mathcal{S}_1}(q_{k-1})) \\ & + \widehat{r} \sum_{k=K_0(z,x)}^{K} (\nu_+)^\top \boldsymbol{h}^{\chi_+^{M_2}}(f(z,\zeta_k)-x)\sigma_2^\top(\boldsymbol{h}^{\mathcal{S}_2}(1-q_{k-1})-\boldsymbol{h}^{\mathcal{S}_2}(1-q_k)) \Bigg\} \end{aligned} \tag{EC.22a}$$

$$\text{s.t.} \quad (54b)-(54h), \tag{EC.22b}$$

where $q_0 = 0$, $q_k = \sum_{j=1}^k p_j$ for $k \in [K]$, we label ζ_k satisfying $f(z,\zeta_k) - x < 0$ with index $k \in \{1,\cdots,K_0(z,x)-1\}$, and for those satisfying $f(z,\zeta_k)-x \ge 0$ by $k \in \{K_0(z,x),\cdots,K\}$. For any fixed (x,z), problem (EC.22) is a bilinear program with linear constraints. The piecewise McCormick relaxation described in Section EC.18 can be applied to approximate this problem.

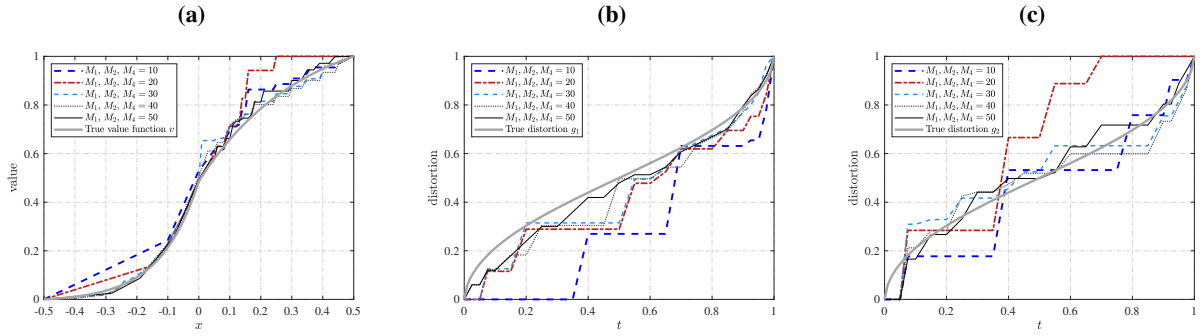
EC.19.1. The Worst-Case Value Function and the Evaluation of PRGSR-CPT

We can evaluate $h_{(\mathbb{V}\mathbb{G}_1\mathbb{G}_2)_M}(\xi - x)$ with different numbers of queries, and obtain the PRGSR-CPT measure $\rho_{(\mathbb{V}\mathbb{G}_1\mathbb{G}_2)_M}(\xi)$ and the worst-case value and distortion functions, where the worst-case functions are obtained by solving subproblem (55) with the optimal solution x of the corresponding PRGSR-CPT model (6). Figure 7 (a) depicts the holistic value functions when $M_1 = M_2 = M_4 = 10, 20, 30, 40, 50$ ($M = M_1 + M_2 + M_3 + M_4$). This shows that the worst-case value function converges

to the true value function. For the change of optimal value functions of $\rho_{(\mathbb{V}\mathbb{G}_1\mathbb{G}_2)_M}(\xi)$, as the number of queries increases, we show the optimal value function and the optimal distortion functions for the case where $\boldsymbol{\sigma}_i = \boldsymbol{\sigma}_i^{\mathrm{AC}}$, $i = 1, 2$, in the objective function of problem (54) in Figure EC.7. The worst-case value function and distortion functions of problem (55) with $N = 5$ are shown in Figure EC.8. Note that the CPT-based shortfall risk of ξ with true functions v^*, g_1^* and g_2^* is 0.2044.

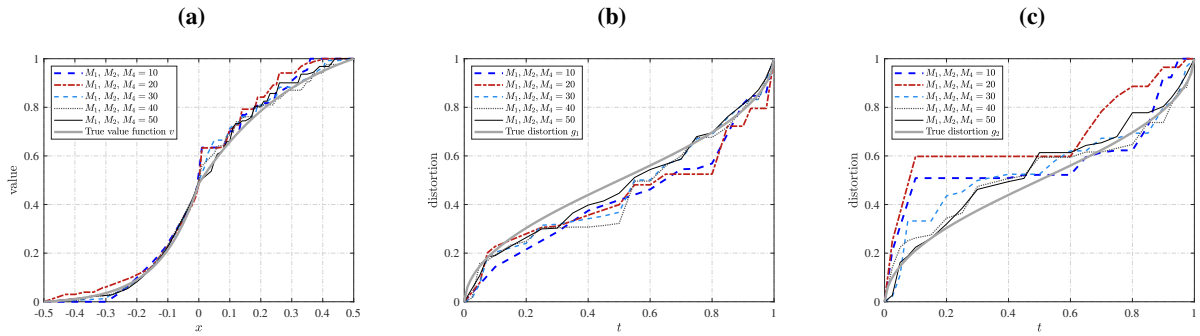
Figure EC.7 shows the change of the optimal value function and the optimal distortion functions as the number of queries (M_1, M_2, M_4) increases from 10 to 50, when $\boldsymbol{\sigma}_i = \boldsymbol{\sigma}_i^{\mathrm{AC}}$, $i = 1, 2$, of problem (54). Figure EC.8 depicts the worst-case value function and distortion functions of problem (55) with the number of pieces of McCormick relaxation being $N = 5$.

Figure EC.7 Worst-Case Value and Distortion Functions with Distortions Fixed at Their Analytic Centers



Note. **(a)** The worst-case value function v. **(b)** The worst-case distortion function g_1. **(c)** The worst-case distortion function g_2. In (a)–(c), the numbers of queries satisfy $M_1 = M_2 = M_4 \in \{10, 20, 30, 40, 50\}$. The worst-case functions are obtained from the optimal solution of problem (54), where $\boldsymbol{\sigma}_1$ and $\boldsymbol{\sigma}_2$ in the objective function are fixed at their analytic centers $\boldsymbol{\sigma}_1^{\mathrm{AC}}$ and $\boldsymbol{\sigma}_2^{\mathrm{AC}}$, respectively.

Figure EC.8 Worst-Case Value and Distortion Functions under the PMR with $N = 5$



Note. **(a)** The worst-case value function v. **(b)** The worst-case distortion function g_1. **(c)** The worst-case distortion function g_2. In (a)–(c), the numbers of queries satisfy $M_1 = M_2 = M_4 \in \{10, 20, 30, 40, 50\}$. The worst-case functions are obtained from the optimal solution of problem (55), where the number of segments in the PMR is $N = 5$.

EC.20. Implications of Using an EUT-Based Polyhedral Method to Elicit CPT Preferences

Consider the case that the DM's preference is characterized by the CPT with true value function v^* and the distortion functions g_1^* and g_2^* defined as in Section 6.1. Suppose that EUT is mistakenly used to model the DM's preference. We develop a modified polyhedral method (see Zhang et al. 2025 for more complicated query selection rules), analogous to that in Section 4.4, to elicit the unknown utility function under the assumption that the distortion function is the identity. The ambiguity set of utility functions is defined as

$$\mathcal{U}_M = \left\{ u_{J_M^{\mathrm{u}}} : [\underline{x}, \bar{x}] \to [0,1] : h_l(\mathbb{E}[u_{J_M^{\mathrm{u}}}(Z_1^l)] - \mathbb{E}[u_{J_M^{\mathrm{u}}}(Z_2^l)]) \le 0,\ l \in [M] \right\},$$

where $h_l = 1$ if $\rho_{\mathrm{CPT}}(Z_1^l) \le \rho_{\mathrm{CPT}}(Z_2^l)$, and $h_l = -1$ otherwise. We now use this ambiguity set to compute the corresponding robust utility-based shortfall of ξ:

$$\inf \left\{ x \in \mathbb{R} : \sup_{u \in \mathcal{U}_M} (\mathbb{E}[u(\xi - x)] - u(0)) \le 0 \right\}. \tag{EC.23}$$

Let $\widetilde{\mathcal{X}}_M^{\mathrm{u}} = \mathcal{X}_M^{\mathrm{u}} \cup \{\xi_k - x\}_{k=1}^K$. Analogous to the computation of PRGSR-CPT in Section EC.12, we apply a bisection method. For each fixed x, the inner problem can be reformulated as

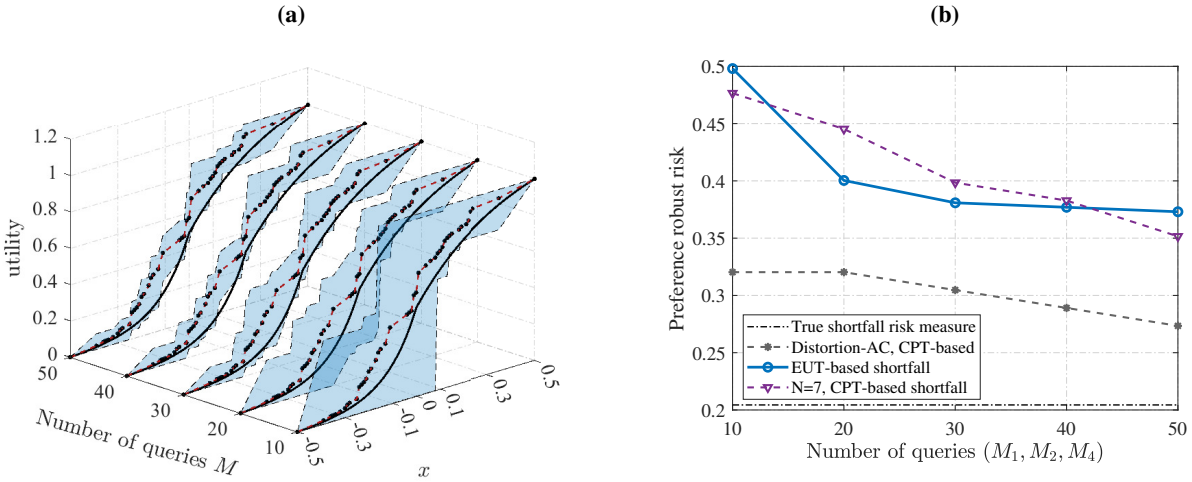
$$\begin{aligned}
&\sup_{\boldsymbol{v}} \sum_{k=1}^{K} (\boldsymbol{R}\boldsymbol{v})^\top \boldsymbol{h}^{\widetilde{\mathcal{X}}_M^{\mathrm{u}}}(\xi_k - x) p_k - (\boldsymbol{R}\boldsymbol{v})^\top \boldsymbol{h}^{\widetilde{\mathcal{X}}_M^{\mathrm{u}}}(0) \\
&\text{s.t. } \boldsymbol{v} \ge 0,\ \boldsymbol{e}^\top \boldsymbol{v} \le 1, \\
&\quad h_m((\boldsymbol{R}\boldsymbol{v})^\top ((1-p^m)\boldsymbol{h}^{\widetilde{\mathcal{X}}_M^{\mathrm{u}}}(r_1^m) + p^m \boldsymbol{h}^{\widetilde{\mathcal{X}}_M^{\mathrm{u}}}(r_3^m) - \boldsymbol{h}^{\widetilde{\mathcal{X}}_M^{\mathrm{u}}}(r_2^m))) \le 0,\ \forall m \in [M].
\end{aligned}$$

The utility-based shortfall can be calculated by the bisection method as described in Section EC.12.

Figure EC.9 (a) shows that when the distortion function is incorrectly fixed as the identity (i.e., under EUT), the true value function lies outside the admissible set of utility functions inferred from the queries when $M \ge 40$. This indicates a misspecification of the preference model. Figure EC.9 (b) further illustrates the impact of this misspecification on the resulting robust shortfall risk measure. When the distortion function is fixed as the identity, the resulting EUT-based robust shortfall is higher than the CPT-based robust shortfall for larger numbers of queries, when $M_4 = 50$ ($M = 50$ for the EUT-based shortfall). In addition, it is also higher than the gray dotted line, which represents the PRGSR-CPT measure obtained by solving the inner problem using the bilinear objective function in (54), with $\boldsymbol{\sigma}_1$ and $\boldsymbol{\sigma}_2$ fixed at $\boldsymbol{\sigma}_1^{\mathrm{AC}}$ and $\boldsymbol{\sigma}_2^{\mathrm{AC}}$, respectively. These observations suggest that ignoring probability distortion leads to a systematic overestimation of the robust shortfall risk. In

contrast, the CPT-based approach, which allows for flexible distortion functions, provides estimates that are closer to the true risk level. Overall, this explains why rejecting the true value function under a misspecified model (EUT) does not imply better estimation accuracy; instead, it reflects model misspecification that leads to biased (conservative) risk evaluation.

Figure EC.9 Range of Utility Functions and Robust Shortfall under EUT and CPT



Note. **(a)** Range of utility functions. The solid line represents the true value function v^*. The shaded region shows the envelope of admissible utility functions over $[-0.5, 0.5]$ induced by $\mathcal{U}_M$ for $M = 10, 20, 30, 40, 50$. **(b)** Robust shortfall under EUT and CPT. The curves show the shortfall risk measure as the number of queries M_4 (with $M_1 = M_2 = M_4$) increases with the number of segments in the PMR being $N = 7$. The horizontal dotted line indicates the true shortfall value, illustrating the higher shortfall risk value using EUT.

EC.21. Qualitative Summary of Convergence of the Estimated Value Function and Distortion Functions

In this section, we provide a qualitative summary and supporting numerical evidence for the convergence behavior of the proposed elicitation procedure. In Section EC.21.1, we quantify the distance from the analytic center to the boundaries of the corresponding polyhedra $\Delta_-^{M_1}$, $\Delta_+^{M_2}$, and Δ_{M_4} defined in (39), (37), and (47) with $m = M_4$. In Section EC.21.2, we evaluate the mean squared distance between the estimated value and distortion functions and their true counterparts.

EC.21.1. Distance from the Analytic Center to the Defining Hyperplanes

Let $\widehat{\Delta}_-^{M_1}$ denote the normalized version of the polyhedron $\Delta_-^{M_1}$ obtained by scaling each constraint so that the corresponding normal vector has unit norm. For simplicity, we write $\widehat{\Delta}_-^{M_1} = \{x : A_i^- x \le b_i^-,\ i \in \mathcal{I}_-\}$. The analytic center of $\widehat{\Delta}_-^{M_1}$ is obtained by solving $\max_x \sum_{i\in\mathcal{I}_-} \log(b_i^- - A_i^- x)$. Let x_-^{AC}

denote the resulting analytic center. The average distance from x_-^{AC} to the defining hyperplanes of $\widehat{\Delta}_-^{M_1}$ is defined as

$$d_{\mathrm{Ave}}^{M_1} = \frac{1}{|\mathcal{I}_-|}\sum_{i\in\mathcal{I}_-}(b_i^- - A_i^- x_-^{\mathrm{AC}}).$$

For the normalized polyhedron $\widehat{\Delta}_+^{M_2} = \{x : A_i^+ x \le b_i^+, i \in \mathcal{I}_+\}$ with analytic center x_+^{AC}, let

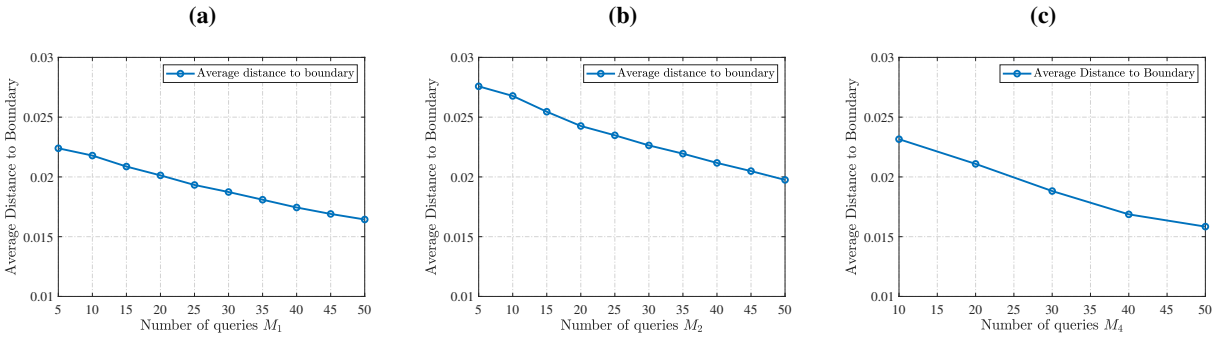
$$d_{\mathrm{Ave}}^{M_2} = \frac{1}{|\mathcal{I}_+|}\sum_{i\in\mathcal{I}_+}(b_i^+ - A_i^+ x_+^{\mathrm{AC}}).$$

For the normalized polyhedron $\widetilde{\Delta}_M^v = \{x : A_i x \le b_i, i \in \mathcal{I}\}$ with $M = M_1 + M_2 + M_3 + M_4$ and analytic center x^{AC}, let

$$d_{\mathrm{Ave}}^{M} = \frac{1}{|\mathcal{I}|}\sum_{i\in\mathcal{I}}(b_i - A_i x^{\mathrm{AC}}).$$

Figure EC.10 depicts the convergence of these distances as the number of queries increases. Specifically, Figure EC.10(a) shows the convergence of the distances from the analytic center to the defining hyperplanes of $\widehat{\Delta}_-^{M_1}$, while Figure EC.10(b) and (c) show the corresponding distances for $\widehat{\Delta}_+^{M_2}$ and $\widetilde{\Delta}_M^v$.

Figure EC.10 Distances from the Elicited Analytic Centers to the Defining Hyperplanes of the Feasible Sets



Note. **(a)** Distance from the elicited analytic center to the defining hyperplanes of $\widehat{\Delta}_-^{M_1}$ as the number of queries M_1 increases. **(b)** Distance from the elicited analytic center to the defining hyperplanes of $\widehat{\Delta}_+^{M_2}$ as the number of queries M_2 increases. **(c)** Distance from the elicited analytic center to the defining hyperplanes of $\widetilde{\Delta}_{M_1+M_2+M_3+M_4}^v$ as the number of queries $M_1 = M_2 = M_4$ increases.

EC.21.2. Mean Squared Distance to the True Functions

To evaluate the estimation accuracy, we measure the mean squared distance between the estimated functions and their true counterparts using randomly generated evaluation points. For a function f and its estimate $\hat{f}$, the error is defined by

$$\mathsf{dl}(f,\hat{f}) = \frac{1}{N}\sum_{i=1}^{N}\left|f(x_i^m) - \hat{f}(x_i^m)\right|^2,$$

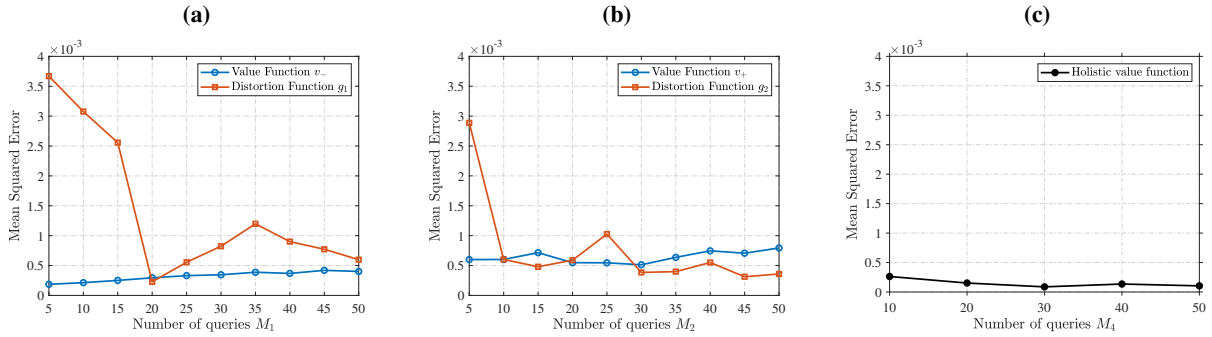
where $\{x_i^m\}_{i=1}^N$ are uniformly generated evaluation points. Throughout the experiments, we set $N = 1000$. Let v_-^*, v_+^*, and v^* denote the true normalized value functions over $[-0.5, 0]$, $[0, 0.5]$, and $[-0.5, 0.5]$, respectively.

Negative value and distortion functions. For the negative part of the value function, evaluation points are generated over $[-0.5, 0]$, while for the distortion function they are generated over $(0, 1)$. Let $(\boldsymbol{c}_{1,-}^{M_1}, \boldsymbol{c}_{2,-}^{M_1})$ denote the analytic center of $\Delta_-^{M_1}$. The corresponding estimated value and distortion functions are given by $v_-^{\mathrm{AC}}(x) = (\boldsymbol{R}\boldsymbol{c}_{1,-}^{M_1})^\top \boldsymbol{h}^{\mathcal{X}_-^{M_1}}(x) - 1$ and $g_1^{\mathrm{AC}}(p) = (\boldsymbol{R}\boldsymbol{c}_{2,-}^{M_1})^\top \boldsymbol{h}^{\mathcal{S}_1}(p)$. Figure EC.11 (a) shows the evolution of the corresponding errors $\mathsf{dl}(v_-^{\mathrm{AC}}, v_-^*)$ and $\mathsf{dl}(g_1^{\mathrm{AC}}, g_1^*)$ as the number of queries increases from 5 to 50. Overall, the estimation error of the distortion function decreases consistently, whereas the improvement for the negative part of the value function is relatively moderate.

Positive value and distortion functions. Let $(\boldsymbol{c}_{1,+}^{M_2}, \boldsymbol{c}_{2,+}^{M_2})$ denote the analytic center of $\Delta_+^{M_2}$. The corresponding estimated value and distortion functions are given by $v_+^{\mathrm{AC}}(x) = (\boldsymbol{R}\boldsymbol{c}_{1,+}^{M_2})^\top \boldsymbol{h}^{\mathcal{X}_+^{M_2}}(x)$ and $g_2^{\mathrm{AC}}(p) = (\boldsymbol{R}\boldsymbol{c}_{2,+}^{M_2})^\top \boldsymbol{h}^{\mathcal{S}_2}(p)$. Figure EC.11 (b) illustrates the convergence of the errors $\mathsf{dl}(v_+^{\mathrm{AC}}, v_+^*)$ and $\mathsf{dl}(g_2^{\mathrm{AC}}, g_2^*)$.

Holistic value function. Let $(\boldsymbol{c}_1^M, \boldsymbol{c}_2^M)$ denote the analytic center of the polyhedron $\widehat{\Delta}^v_{M_1+M_2+M_3+M_4}$. To evaluate the error of the overall value function $v^{\mathrm{AC}}(x) = \left(\frac{1}{1+\widehat{r}}\boldsymbol{R}\boldsymbol{c}_1^M, \frac{\widehat{r}}{1+\widehat{r}}\boldsymbol{R}\boldsymbol{c}_2^M\right)^\top \boldsymbol{h}^{\mathcal{X}_{M_4}}(x)$, we generate evaluation points uniformly over $[-0.5, 0.5]$. The resulting error $\mathsf{dl}(v^{\mathrm{AC}}, v^*)$ is shown in Figure EC.11 (c).

Figure EC.11 Mean Squared Errors of the Estimated Distortion and Holistic Value Functions



Note. **(a)** Mean squared errors of the estimated distortion function g_1 obtained from the analytic center of polyhedron $\widehat{\Delta}_-^{M_1}$. **(b)** Mean squared errors of the estimated distortion function g_2 obtained from the analytic center of polyhedron $\widehat{\Delta}_+^{M_2}$. **(c)** Mean squared error of the estimated holistic value function v obtained from the analytic center of polyhedron $\widehat{\Delta}^v_{M_1+M_2+M_3+M_4}$. Here, M_1, M_2, M_3, and M_4 denote the numbers of queries of Types 1–4, respectively. In particular, for $M_4 \in \{10, 20, 30, 40, 50\}$, we set $M_1 = M_2 = M_4$. The construction of $\widehat{\Delta}^v_{M_1+M_2+M_3+M_4}$ relies on $\widehat{\Delta}^{v-v+}_{M_1+M_2+M_3+M_4}$, where the estimators $\widehat{g}_1$ and $\widehat{g}_2$ are defined as in (40).

The numerical results indicate that the proposed polyhedral elicitation method successfully reduces estimation error but also appears to stabilize after some number of queries. For $\Delta_{-}^{M_1}$, the estimation error appears to become stable after approximately 35 questions of Type 1, while it is around 20 questions for the estimation of the holistic value function. These results suggest that while our elicitation may eventually produce high-accuracy functions, further reductions in estimation error may require additional queries.

EC.22. Comparative Analysis of Trade-offs with Standard Parametric Approach

We have also undertaken some comparative analysis between our method and a standard parametric approach where the true value/distortion functions are not necessarily parametric. We consider a parametric family commonly used in CPT (see Table 1). Since the true preference functions may not belong to this parametric family (a situation we refer to as the model being misspecified), the fitted functions may deviate from the true ones even when the parameters are optimally estimated.

Specification of a parametric family. We consider the following family of parametric value functions:

$$\widetilde{v}(x;\alpha,\beta,\lambda)=\begin{cases} x^{\alpha}, & x\geq 0,\\ -\lambda(-x)^{\beta}, & x<0,\end{cases} \tag{EC.24}$$

and distortion functions:

$$\widetilde{g}_1(t;\delta_1,\gamma_1)=\exp(-\delta_1(-\ln t)^{\gamma_1}), \qquad \widetilde{g}_2(t;\delta_2,\gamma_2)=\exp(-\delta_2(-\ln t)^{\gamma_2}), \tag{EC.25}$$

where $\alpha,\beta\in[0,1]$, $\delta_k\in[0,2]$, and $\gamma_k\in[0,2]$ for $k=1,2$.

Estimation of the Parameter. To estimate the parameters of the value function, we first normalize the elicited value function over the interval $[-0.5,0.5]$. Preference queries provide observations $v_i^M=\left(\frac{1}{1+\widehat{r}}\boldsymbol{R}\boldsymbol{c}_1^M,\frac{\widehat{r}}{1+\widehat{r}}\boldsymbol{R}\boldsymbol{c}_2^M\right)^{\top}\boldsymbol{h}^{\mathcal{X}_{M_4}}(x_i)$ at selected points $x_i\in\mathcal{X}_M$ obtained by the analytic center $(\boldsymbol{c}_1^M,\boldsymbol{c}_2^M)$ of the polyhedron $\widehat{\Delta}^v_{M_1+M_2+M_3+M_4}$. The parameters (α,β,λ) are estimated by solving the following mean squared error problem:

$$\begin{aligned}\min_{\alpha,\beta\in[0,1],\tau\in[0,2],\lambda\tau\in[0,2]}\ &\sum_{i=1}^{J}\left(\tau\widetilde{v}(x_i;\alpha,\beta,\lambda)-v_i^M\right)^2\\ \text{s.t.}\ &\tau\left(\widetilde{v}(\bar{x})-\widetilde{v}(\underline{x})\right)=1,\end{aligned} \tag{EC.26}$$

where the scaling parameter τ is introduced to align the parametric value function with the normalized elicited value function. Similarly, the parameters (δ_k,γ_k) of the distortion functions are estimated via nonlinear least squares. The elicited values are obtained from the analytic center

$(\boldsymbol{c}_{-,1}^{M_1}, \boldsymbol{c}_{-,2}^{M_1})$ of the polyhedron $\Delta_-^{M_1}$ as $g_{1,j}^{M_1} = (\boldsymbol{R}\boldsymbol{c}_{-,2}^{M_1})^\top \boldsymbol{h}^{S_1}(p_j)$. Likewise, the elicited values of $g_{2,j}^{M_2} = (\boldsymbol{R}\boldsymbol{c}_{+,2}^{M_2})^\top \boldsymbol{h}^{S_2}(p_j)$ are obtained from the analytic center $(\boldsymbol{c}_{+,1}^{M_2}, \boldsymbol{c}_{+,2}^{M_2})$ of polyhedron $\Delta_+^{M_2}$. We solve the following regression problems:

$$\begin{aligned} &\min_{\delta_1,\gamma_1\in[0,2]} \sum_{j=1}^{S} \left(\exp\left(-\delta_1(-\ln p_j)^{\gamma_1}\right) - g_{1,j}^{M_1}\right)^2, \\ &\min_{\delta_2,\gamma_2\in[0,2]} \sum_{j=1}^{S} \left(\exp\left(-\delta_2(-\ln p_j)^{\gamma_2}\right) - g_{2,j}^{M_2}\right)^2. \end{aligned} \tag{EC.27}$$

Let $(\alpha^*, \beta^*, \lambda^*)$ and (δ_k^*, γ_k^*), $k = 1, 2$, denote optimal solutions to problems (EC.26) and (EC.27), respectively.

Evaluation metric. To quantify the discrepancy between the estimated parametric functions and the true preference functions, we use the mean squared error evaluated over randomly generated points. For the distortion functions, the error is defined as

$$\mathsf{dl}(\widetilde{g}_k(\cdot;\delta_k^*,\gamma_k^*), g_k) = \frac{1}{N}\sum_{i=1}^{N} |\widetilde{g}_k(t_i^m;\delta_k^*,\gamma_k^*) - g_k(t_i^m)|^2,\ k = 1, 2,$$

where $\{t_i^m\}_{i=1}^N$ are uniformly drawn from $(0, 1)$. For the value function, let

$$\mathsf{dl}(\widetilde{v}(\cdot;\alpha^*,\beta^*,\lambda^*), v^*) = \frac{1}{J}\sum_{i=1}^{J} |\widetilde{v}(x_i^m;\alpha^*,\beta^*,\lambda^*) - v^*(x_i^m)|^2,$$

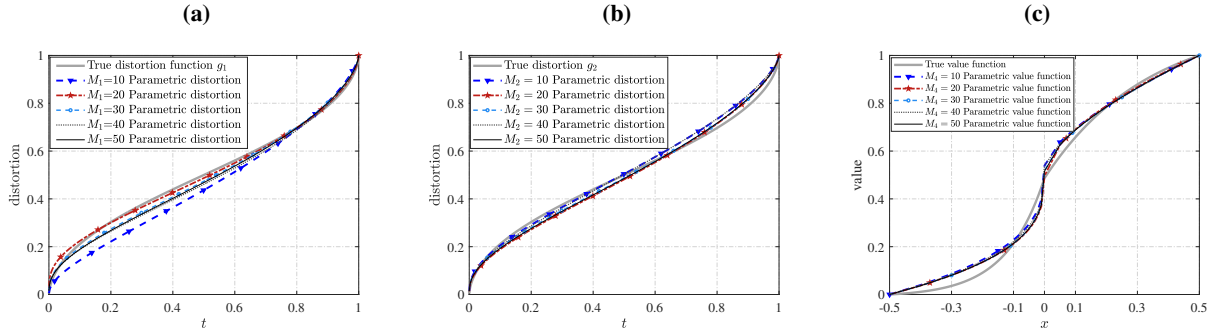
where $\{x_i^m\}_{i=1}^J$ are uniformly drawn from $[-0.5, 0.5]$. Throughout the experiments, we set $N = 1000$ and $J = 1000$. For comparison, we also implement a parametric benchmark, where the functional forms of the value and distortion functions are assumed to be correctly specified (see Section 6.1). The parameters are estimated by solving (EC.26) and (EC.27), which yields the minimum achievable approximation error under the assumed parametric specification.

Comparative analysis. Figure EC.12 depicts the estimated distortion and the value functions based on $\Delta_-^{M_1}$, $\Delta_+^{M_2}$, and $\Delta_{M_1+M_2+M_3+M_4}^{v}$, respectively. The parametric CPT specification produces smooth functional forms but may deviate from the true functions due to model misspecification. In contrast, the nonparametric polyhedral approach more closely tracks the true preference functions, although small local fluctuations may appear as a consequence of the polyhedral elicitation procedure.

Figure EC.13 further reports the evolution of the mean squared error as the number of queries increases. The results show that the parametric method achieves similar performance in terms of distortion function quality, while demonstrating a clear improvement in terms of the quality of

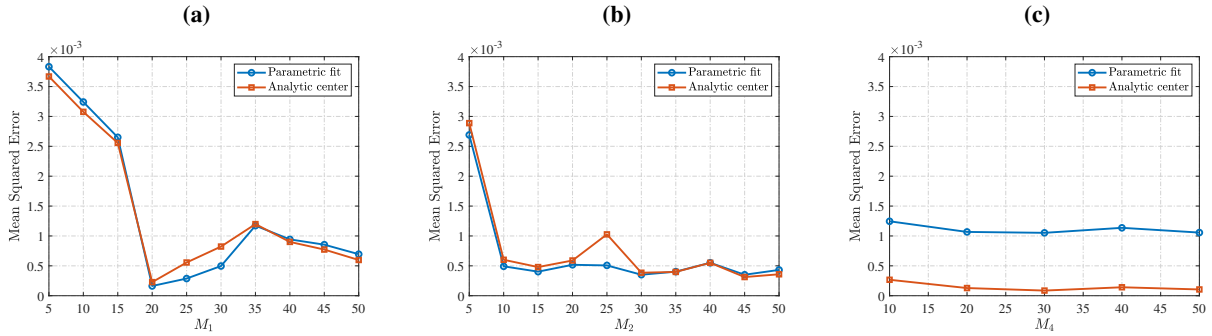
the holistic value functions v. We attribute the latter loss in performance to the misspecification of the parametric family for $\tilde{v}$. Based on the test results, we conclude that the performance of the parametric approach is subject to model misspecification and estimation error, highlighting the advantages of the nonparametric polyhedral method.

Figure EC.12 Parametric Estimation of the Distortion and Holistic Value Functions



Note. **(a)** Parametric Estimation of $\widetilde{g}_1(\cdot;\delta_1,\gamma_1)$ using function values derived from the analytic center of the polyhedron $\Delta_-^{M_1}$. **(b)** Parametric Estimation of $\widetilde{g}_2(\cdot;\delta_2,\gamma_2)$ using function values derived from the analytic center of the polyhedron $\Delta_+^{M_2}$. **(c)** Parametric Estimation of $\widetilde{v}(\cdot;\alpha,\beta,\lambda)$ using the function values derived from the analytic center of the polyhedron $\widehat{\Delta}_{\boldsymbol{M}}^{v}$ (the projection of $\widehat{\Delta}_{\boldsymbol{M}}$ onto the space of $(\boldsymbol{R}\widetilde{\boldsymbol{v}}_-, \boldsymbol{R}\widetilde{\boldsymbol{v}}_+)$). In (a)–(c), the black solid curve represents the true functions, while the dashed curves represent the estimated parametric functions.

Figure EC.13 Mean Squared Errors of Parametric and Nonparametric Preference Estimators



Note. **(a)** Evolution of the mean squared error for g_1 as the number of queries M_1 increases. **(b)** Evolution of the mean squared error for g_2 as the number of queries M_2 increases. **(c)** Evolution of the mean squared error for v as the number of queries M_4 increases. In (a)-(c), the blue curve corresponds to the parametric estimation and the orange curve corresponds to the nonparametric (polyhedral) estimation. Both estimators improve as the number of queries increases. The nonparametric estimator generally achieves lower error in the large-sample regime, as illustrated when $M_1 \geq 35$, $M_2 \geq 40$, and across all tested values of M_4.

EC.23. Extended Concluding Remarks

In this section, we provide additional details on the implementation and limitations of the proposed models and CPT-based preference elicitation approaches, as well as their application to optimal decision-making problems.

(i) In practice, the only directly observable data are historical realizations of ξ and $\boldsymbol{\zeta}$, whereas the support of the random variable ξ and random vector $\boldsymbol{\zeta}$ are not directly observable. However, the support set of ξ or $\boldsymbol{\zeta}$ can often be inferred from domain-specific knowledge (e.g., the random loss ξ is nonnegative and is upper bounded, and the random return rates $\boldsymbol{\zeta}$ can be supposed bounded); it may also be constructed from historical data (e.g., the convex hull of all historical realizations of ξ and $\boldsymbol{\zeta}$ respectively).

(ii) There is a limitation in the developed models and preference elicitation approaches, that is, we are unable to use the CPT-based shortfall risk measure to elicit the DM's risk preference directly; rather we have to use the distorted expected values of the random prospects, that is, $\mathbb{E}_{g_1 g_2}[v(\cdot)]$ to elicit the DM's preference via pairwise comparison questionnaires.

(iii) Weak preferences are unavoidable under the current questionnaire design. When the expected values of two lotteries are very close, the decision maker may not show a strong preference. The weak preferences may affect the correctness of the added inequality. Due to rounding of the generated cut points r_1, r_2, r_3, the sign of the newly added constraint in the ambiguity set may be reversed. To tackle the issue, one may incorporate the robust approaches Bertsimas and O'Hair (2013). We leave this for future exploration.

(iv) The robust model, preference elicitation approaches and the formulations discussed in this paper can be easily applied to one-stage decision-making problems with a CPT-based objective:

$$\text{(PRO-CPT)} \qquad \max_{z\in Z} \min_{(v,g_1,g_2)\in \mathbb{V}\mathbb{G}_1\mathbb{G}_2} \mathbb{E}_{g_1 g_2}[v(f(z,\boldsymbol{\zeta}))], \tag{EC.28}$$

where $\mathbb{V}\mathbb{G}_1\mathbb{G}_2$ is the ambiguity set of (v, g_1, g_2). Specifically, we may begin by obtaining an ambiguity set $(\mathbb{V}_-\mathbb{G}_1)_M$ and $(\mathbb{V}_+\mathbb{G}_2)_M$ of (v_-, g_1) and (v_+, g_2) of the true value functions respectively using the modified polyhedral method presented in Section 4.2.1. Then we can use the by-product, estimate $\widehat{g}_1$ and $\widehat{g}_2$ to construct the ambiguity set of the normalized value function v over $[\underline{x}, \bar{x}]$ with M pairs of queries to elicit the range of the potential ratio r (see Section 4.4). Consequently, we use $(\mathbb{V}_-\mathbb{G}_1)_M$, $(\mathbb{V}_+\mathbb{G}_2)_M$ and the range of r to construct $(\mathbb{V}\mathbb{G}_1\mathbb{G}_2)_M$. Then we can consider the following simplified preference robust optimization model:

$$\text{(PRO-CPT-S)} \qquad \vartheta := \max_{z\in Z} \min_{(v,g_1,g_2)\in (\mathbb{V}\mathbb{G}_1\mathbb{G}_2)_M} \mathbb{E}_{g_1 g_2}[v(f(z,\boldsymbol{\zeta}))]. \tag{EC.29}$$

Analogous to discussions in Section EC.19, we can use $(\mathbb{V}_J\mathbb{G}_{N_1}\mathbb{G}_{N_2})_M$ to approximate the ambiguity set $(\mathbb{V}\mathbb{G}_1\mathbb{G}_2)_M$, and then consider the approximate preference robust optimization model:

$$\text{(PRO-CPT-S-J)} \qquad \vartheta_{JN} := \max_{z\in Z} \min_{(v,g_1,g_2)\in(\mathbb{V}_J\mathbb{G}_{N_1}\mathbb{G}_{N_2})_M} \mathbb{E}_{g_1g_2}[v(f(z,\zeta))]. \tag{EC.30}$$

For each fixed decision vector z, the inner minimization problem as a bilinear program with linear constraints and can be approximated using the piecewise McCormick relaxation described in Section EC.18. The error arising from the approximation can be quantified as in Guo et al. 2024. In comparison with the expected utility maximin problem in Hu et al. 2025, Armbruster and Delage 2015, Guo et al. 2024 and the preference robust distortion risk measure in Wang and Xu (2023), the preference robust optimization model (EC.28) covers a larger class of problems where the DM's preference is represented by CPT.

References

Armbruster B, Delage E (2015) Decision making under uncertainty when preference information is incomplete. *Management Science* 61(1):111–128.

Bertsimas D, O'Hair A (2013) Learning preferences under noise and loss aversion: An optimization approach. *Operations Research* 61(5): 1190–1199.

Boyd S, Vandenberghe L (2004) *Convex Optimization* (Cambridge University Press).

Chen H, Sun XA, Yang H (2024) Robust optimization with continuous decision-dependent uncertainty. *SIAM Journal on Optimization* 33(3):2406–2434.

Guo S, Xu H, Zhang S (2024) Utility preference robust optimization with moment-type information structure. *Operations Research* 72(5): 2241–2261.

Hu J, Zhang D, Xu H, Zhang S (2025) Distributional utility preference robust optimization models in multi-attribute decision making. *Mathematical Programming* 212: 519–565.

Mao T, Cai J (2018) Risk measures based on behavioural economics theory. *Finance and Stochastics* 22:367–393.

Wang W, Xu H (2023) Preference robust distortion risk measure and its application. *Mathematical Finance* 33(2):389-434.

Zhang, S., Guo, S., Sim, M. and Xu, H. (2025) Modified Polyhedral Method for Elicitation of Shape-Free Utility and Conservatism Reduction in Robust Optimization. arXiv preprint arXiv:2503.23269. Available at `https://arxiv.org/abs/2503.23269` (Accessed 2025).